scientific reports

Check for updates

OPEN

Mucosomes as next-generation drug carriers for treating mucus-resident bacterial infections and biofilms

Giuseppe Guagliano[1], Emanuela Peluso[2], Cosmin Stefan Butnarasu[3], Elisa Restivo[2], Lorenzo Sardelli[1], Enrica Frasca[1], Paola Petrini[4], Nicola Tirelli[5], Stefania Sganga[5], Livia Visai[2,6]✉ & Sonja Visentin[1]✉

Deaths connected to bacterial infections are expected to outnumber those caused by cancer by 2050. Multiple advantages, including enhanced efficacy of the treatment, characterize the use of nanocarriers to deliver antibiotics. This work explores the use of mucosomes – intrinsically glycosylated mucin nanoparticles – to deliver ciprofloxacin to fight *Pseudomonas aeruginosa* and *Staphylococcus aureus* infections. Mucins are a family of glycoproteins representing the major non-aqueous component of human mucus and are known for actively interacting with bacteria, reducing their virulence, and limiting their aggregations. This study shows that these critical properties of mucin are preserved in mucosomes, enabling a strong synergy with the loaded antimicrobial drug. Empty mucosomes exert a bacteriostatic activity, inhibiting bacterial growth up to 70%. Ciprofloxacin-loaded mucosomes were able to decrease the minimum inhibitory concentration of ciprofloxacin against *S. aureus* by up to 50%. Mucosomes could prevent biofilm formation and disassemble well-established biofilms by reducing the biomass by up to 98%. Mucosomes further facilitated the transmucosal delivery of ciprofloxacin in a 3D mucus-mimicking model. These results, together with the possibility of freeze-drying and storing drug-loaded mucosomes without impairing their efficacy, suggest the suitability of this approach to tackle mucosal bacterial infections. Interestingly, this nanosystem has been shown to enhance the phagocytic action of blood in eradicating bacterial biofilms.

Keywords Mucin, Mucosa, Infections, Drug delivery, Ciprofloxacin, Nanoparticles, Glycans

According to the World Health Organization, deaths caused by bacterial infections are expected to outnumber those caused by cancers by 2050[1]. This concerning trend is empowered by antimicrobial resistance (i.e., the ability of bacteria to progressively tolerate the administration of a given antimicrobial active principle), as well as by the "discovery void" of novel antimicrobial molecules[2–5].

Among the different scenarios where bacterial infections can develop, mucosal tissues are a frequent target as they represent the primary interface between the inner tissues and the external environment[6,7]. In the mucosa, the very first line of defense is represented by mucus, a hydrogel that moisturizes and lubricates all the wet epithelia of the human organism[8–12]. Mucus acts as a barrier that can trap the invaders, preventing them from reaching the epithelia, and can clear them through tightly regulated self-renewal mechanisms[13]. However, there are multiple situations in which these physiological defensive functions are impaired, resulting in the establishment of challenging mucosal infections[10,14,15].

[1]Department of Molecular Biotechnology and Health Sciences, University of Torino, via Nizza 44bis, Turin 10126, Italy. [2]Molecular Medicine Department (DMM), Operative Unit (OU) Interuniversity Center for the Promotion of the 3Rs Principles in Teaching and Research (Centro 3R), Centre for Health Technologies (CHT), Unità di Ricerca (UdR) INSTM, University of Pavia, Pavia 27100, Italy. [3]Institute of Pharmacy Biopharmaceuticals, SupraFAB, Freie Universität Berlin, Altensteinstr 23a, 14195 Berlin, Germany. [4]BioAvatar Lab, Department of Chemistry, Materials, and Chemical Engineering "G. Natta", Politecnico di Milano, Piazza L. Da Vinci 33, Milan 20133, Italy. [5]Laboratory of Polymers and Biomaterials, Fondazione Istituto Italiano di Tecnologia, Via Morego 30, Genova 16163, Italy. [6]UOR6 Nanotechnology Laboratory, Department of Prevention and Rehabilitation in Occupational Medicine and Specialty Medicine, Istituti Clinici Scientifici Maugeri IRCCS, Via Maugeri 4, Pavia 27100, Italy. ✉email: livia.visai@unipv.it; sonja.visentin@unito.it

A glaring example is represented by pulmonary infections contributing to bronchiectasis, chronic obstructive pulmonary disease, or cystic fibrosis[15–17]. These diseases are characterized by the secretion of a thicker and more viscous layer of mucus that the physiological mucociliary mechanisms cannot clear[18]. In these conditions, mucus switches from an effective barrier to a stagnating environment, suitable for bacteria to proliferate safely by providing them with a confined matrix rich in nutritious compounds[19–21]. Moreover, such a thicker and more viscous layer of mucus impairs the possibility of the drugs reaching their targets. The combination of these effects culminates in the settlement of resilient bacteria that form biofilms, which are complex communities, encased in a self-produced extracellular polymeric substance (EPS). The EPS matrix, composed of polysaccharides, proteins, and extracellular DNA, has been shown to have several functions[22]. Firstly, it shields the bacterial cells from direct interaction with the immune system phagocytes (macrophages and neutrophils). Secondly, it inhibits the diffusion of antimicrobial agents and reactive oxygen species (ROS). This protective layer reduces the efficacy of phagocytosis by limiting the recognition and binding of immune cells to bacterial antigens, which is carried out through specific patterns[23]. As a result, infections associated with biofilms are challenging to eliminate. The successful eradication of biofilm infections is well-known for being particularly challenging, especially when biofilms are formed within the viscous 3D matrix of pathological mucus (as it happens frequently in the case of cystic fibrosis)[24–26]. Biofilm treatment requires intensive care, with prolonged and multiple antibiotic treatments, which are mostly directed at mitigating exacerbation rather than resolving the chronic infection[27–29]. These combined effects were previously modeled with in vitro tools reproducing the key features of cystic fibrosis mucus, including those governing drug diffusion, bacterial aggregation, and distribution[10].

There is a common consensus that mucosal administration holds the potential to enhance the efficacy of numerous drugs while having higher patient acceptance[30–32]. Mucosal drug delivery is still challenging as pathological mucus can sterically and interactively hinder drug diffusion[30–32]. The key to bypassing such a barrier resides in formulating mucoadhesive and mucopenetrating formulations[30–32]. The combination of these two properties would maximize the diffusion of drugs through mucus while minimizing its barrier effect, leading to the enhancement of systemic drug absorption[30–32]. Aiming to fulfill these requirements and maximize the outcomes of mucosal administration, several material-based drug delivery systems – in the form of polymeric nanocarriers – have been engineered in recent years[30–32]. However, all these systems share the need to be functionalized (e.g., thiolation) to be able to positively interact with the mucus layer[30,33]. The intrinsic complexity behind these functionalizations represents a substantial limitation to scaling up the production and clinical application of mucoadhesive and mucopenetrating delivery systems[31].

We recently developed mucosomes, a nanoparticle-based drug delivery system designed to address the unique challenges posed by the mucus barrier[34]. Mucosomes are bioinspired from human mucus and engineered to adhere to the mucus matrix, allowing for sustained drug release and increased local drug concentrations at the site of action[34]. This may significantly improve therapeutic efficacy while potentially reducing systemic side effects. A wide range of therapeutic agents, including small molecules, biologics (e.g., antibodies, peptides), and even nucleic acid mimetics, can be loaded into mucosomes[34]. Such flexibility could provide opportunities for the management of a variety of acute and chronic diseases. Notably, mucosomes can be synthesized, loaded with the therapeutic compound, and naturally functionalized with surface glycans in a single one-pot reaction, eliminating the need for additional synthetic glycan modifications due to the intrinsic glycosylation of mucins[34].

This paper provides a proof of concept of the efficacy of drug-loaded mucosomes for fighting mucus-resident bacterial infections. We employed two clinically relevant, biofilm-forming bacterial strains present in chronic airway infections, the Gram-negative *Pseudomonas aeruginosa* and the Gram-positive *Staphylococcus aureus*. We focused on the ciprofloxacin case study, as a broad-spectrum antibiotic, acting against both bacterial strains. This study aimed to investigate the feasibility of loading mucosomes with ciprofloxacin and evaluate the efficacy of the resulting nanosystem, even in a more complex 2D system that involves the action of human blood. Our focus was on examining the ability of mucosomes to selectively target bacteria within a 3D chronic infection mucus model and disrupt biofilm formation.

Experimental section

Preparation and characterization of mucosomes

Synthesis of mucosomes

Mucosomes were prepared as previously described through a desolvation method[24]. Briefly, porcine gastric mucin (PGM) (CAS #84082-64-4, Merck, DE) was dissolved at a final concentration of 25 mg/mL in 10 mM NaCl and homogenized by magnetic stirring for 1 h. The pH of the suspension was adjusted to 8.5-9.0 with 1 M NaOH. Desolvation was induced with ethanol (CAS #64-17-5, Merck, DE) added at approximately 1 mL/min until PGM reached a final concentration of 5 mg/mL. Addition of ethanol induced aggregation of PGM into nanoparticles and subsequent precipitation; glutaraldehyde was then added to crosslink the PGM nanoparticles, reaching the final concentration of 0.072% (w/v). PEG 6000 (CAS #39927-08-7, Merck, DE) was added at the final concentration of 2% (w/v) to the mixture to prevent mucosomes aggregation. Mucosomes were finally purified through 3 cycles of centrifugation at 10,000 RPM for 20 min at 4 °C. After each cycle the supernatant was discarded, and the pellet was resuspended in mQ water. After the final cycle, no resuspension was performed, and the pellets were stored at 4 °C either directly or after having been freeze-dried overnight.

To produce loaded mucosomes, either ciprofloxacin (CAS #1216659-54-9, Merck, DE) or fluorescein 5(6)-isothiocyanate (FITC) (CAS #27072-45-3, Merck, DE) was solubilized and mixed with the initial mucin suspension just before the desolvation step. The efficiency of the encapsulation (EE) process was indirectly estimated by quantifying the drug in the supernatants during the purification process, as in Eq. 1.

$$EE = 100 \times \frac{Drug\ in\ supernatant\ [mg]}{Total\ drug\ [mg]} \quad (1)$$

The amount of FITC in the supernatant was detected by fluorescence spectroscopy using a Horiba Jobin Yvon Fluorolog 3 TCSPC fluorometer equipped with a 450 W xenon lamp and a Humamatsu R928 photomultiplier. FITC was excited at 490 nm and detected at 520 nm. The ciprofloxacin in the supernatant volume was measured via UV-spectroscopy by measuring the absorbance of the samples at 324 nm. The amount of ciprofloxacin in the supernatant volume was quantified using a 7-point calibration curve ($R^2 = 0.99$, plotted in the Supporting Information).

Drug release from Ciprofloxacin-loaded mucosomes

An 800 µL suspension in phosphate-buffered saline (PBS) of mucosomes (1.6 mg/mL) loaded with ciprofloxacin (final concentration of 400 µg/mL) was placed into dialysis Eppendorf tubes with a molecular weight cut-off (MWCO) of 3.5 kDa (Pur-A-Lyzer™ Midi Dialysis Kit, Merck). The Eppendorfs containing the loaded mucosomes were then immersed in Falcon tubes filled with 15 mL of PBS (pH 7.4) and incubated at 37 °C. At predetermined time intervals (0.5, 1, 2, 4, 6, 8, 24, 48, and 72 h), the PBS from the tubes was collected and replaced with 15 mL of fresh PBS. The concentration of ciprofloxacin released from the mucosomes was quantified by measuring the absorbance of the collected PBS at 324 nm by UV spectrometry.

Physico-chemical characterization of mucosomes

Transmission electron microscopy TEM samples were prepared by drop-coating the empty and ciprofloxacin-loaded mucosomes at a concentration of 3 mg/mL in water, into the carbon-coated copper grid. Observations were performed with a JEM 1200 EX II (JEOL, Peabody, MA, USA) TEM operating at 100 kV and equipped with a MegaView G2 CCD camera (Olympus OSIS, Tokyo, Japan). Images were acquired at 100 k×.

Nanoparticle tracking analysis For batch analyses, a 5 mg/mL mucosome dispersion was diluted to 0.05 mg/mL in 10 mM NaCl and analyzed on a Nanosight NS300 instrument (Malvern Panalytical) using flow index 50, camera level 16, screen gain 1, and threshold 4. For on-line analyses, a 5 mg/mL mucosome dispersion was injected as such, but during the AF4 separation experienced roughly a 1:100 dilution, so that the actual concentration analyzed was about 0.05 mg/mL, which allowed to sample the AF4 flow and connect it to an at-line NTA (scattering mode - withdraw index of 80, camera level 16, screen gain 1, threshold 4; fluorescence (excitation laser 488 nm) mode = same, but screen gain 2).

Asymmetric flow Field-Flow fractionation (AF4) The AF4 system AF2000 TM (Postnova Analytics, Landsberg, Germany) was coupled online to - in the following order − 1) a Dawn Heleos II multi-angle sttic light scattering (SLS, also known as MALS) (Wyatt technology, Santa Barbara, California) for radius of gyration (Rg) determination (static light scattering, SLS), 2) a Möbiuz dynamic light scattering autocorrelator (Wyatt technology) connected to the 12th angle of the Dawn for hydrodynamic radius (RH) determination, 3) an Optilab T-Rex refractive index (Wyatt technology) detector for concentration determination, 4) an NTA (Nanosight NS300, Malvern Panalytical) for hydrodynamic radius of just fluorescent mucosomes. The AF4 frit-inlet channel was equipped with a 350 µm spacer and a 10 kDa MWCO membrane made of regenerated cellulose as an accumulation wall. A 10 mM sodium chloride solution in MilliQ water was filtered through a 0.1 µm filter and used as an eluent. In a typical experiment, the detector flow rate was set at 0.5 mL/min, and 50 µL of sample (mucosomes 5 mg/mL) were injected setting 0.2 mL/min as the injection flow rate. For the elution step, the cross flow was maintained constant at 1 mL/min for 10 min and then exponentially (exponent = 0.10) decreased to 0 mL/min over 40 min, subsequently it was kept at 0 mL/min for an additional 10 min. Last, a rinse step (i.e., cross flow at 0 mL/min and purge valve on) was performed for 1 min. The data collected by the SLS and refractive index detectors were analyzed on ASTRA software (Wyatt technology) and fitted with a Zimm model using a dn/dc of 0.144 (mL/g).

Permeability assessment through a mucus-like membrane

Permeability through permeapad® membranes Permeability measurements of the released ciprofloxacin were assessed using the bio-mimetic permeability platform PermeaPad®. Ciprofloxacin stock solutions were initially prepared at a concentration of 10 mg/mL in DMSO. The stock solutions were then diluted with a 10 mM phosphate buffer (PBS) (pH 7.4, 10 mM) to obtain working solutions at concentrations of 500 µM. Similarly, suspensions in PBS (pH 7.4, 10 mM of nanoparticles loaded with ciprofloxacin - final concentration of 500 µM) were prepared as outlined in Sect. "Synthesis of mucosomes".

Before permeability measures, the PermeaPad® membrane was equilibrated with 400 µL of PBS added in the acceptor compartments and stored for 1 h at room temperature. Then, the PBS was replaced with either a solution of ciprofloxacin or ciprofloxacin-loaded NPs suspension (both at 500 µM), while 200 µL of fresh PBS was added to the acceptor chambers. The donor and acceptor plates were coupled and incubated for 5 h at room temperature. Upon incubation, samples were collected from each acceptor compartment, and the concentration of ciprofloxacin was analyzed by HPLC-UV (Agilent, Varian ProStar). The quantification was carried out at 324 nm, using a 7-points calibration standard curve ($R^2 = 0.99$), to determine the ciprofloxacin concentrations.

The apparent permeability coefficient (P_{app}) for each compound was calculated using Eq. 2 derived from Fick's law for steady-state conditions.

$$P_{app} = \frac{\left(\frac{dQ}{dt}\right)}{(C_0 \times A)} \quad (2)$$

where dQ represents the amount of drug (in moles) that permeated into the acceptor compartment over the time interval dt (18,000 s), C_0 is the initial donor concentration, and A is the surface area of the well membrane (0.15 cm^2). Caffeine was considered as a reference standard to confirm the integrity of different PermeaPad® plates.

Permeability through a cystic fibrosis pulmonary mucus model Permeability through a cystic fibrosis (CF) mucus model was estimated as previously described[12]. Briefly, an alginate-mucin hydrogel as in vitro model of the CF mucus was produced through internal gelation. To this end, a solution of mucin at the concentration of 43.7 mg/mL, a solution of alginate (CAS #9005-38-3, Merck, DE) at the concentration 21 mg/mL, a suspension of $CaCO_3$ (CAS #471-34-1, Merck, DE), at the concentration of 7 mg/mL, and a solution of glucono-delta-lactone (CAS #90-80-2, Merck, DE) were prepared. Mucin, alginate, and $CaCO_3$ powders were disinfected before use by exposure to UV light for 1 h, under a laminar-flow hood. GDL solution was sterilized through filtration with a 0.22 µm syringe filter. To produce the hydrogel, 4 parts of mucin solution were first mixed with 1 part of alginate solution; 1 part of $CaCO_3$ solution was then added and homogeneously mixed before 1 part of GDL solution was finally added to initiate the dissolution of $CaCO_3$ and crosslinking. Immediately after the addition of GDL, 40 µL of the mixture were pipetted on the bottom of Transwell® inserts for 24-well plates (Corning, USA). The loaded inserts were transferred into a proper multiwell plate and stored at 4 °C for 20 h before being used allowing the complete crosslinking of the mucus-like hydrogel.

The percent change in P_{app} values between the PermeaPad® alone and the integrated PermeaPad® + mucus system was calculated as detailed in Eq. 3.

$$\Delta P = \frac{(P_{app} - P_{app\,(mucus)})}{P_{app}} \quad (3)$$

Preparation of mucosomes for in vitro tests
Ciprofloxacin-loaded mucosomes were resuspended in PBS to reach a final concentration of ciprofloxacin of 2290.5 µg/ml. This stock suspension was then diluted in Müller-Hinton (MH) broth medium to reach a concentration of 512 µg/ml, representing the working NPs suspension at the highest concentration of ciprofloxacin. NPs suspensions at lower concentrations of ciprofloxacin were obtained through serial dilutions in MH. Similarly, empty mucosomes and FITC-loaded mucosomes were resuspended in PBS to reach the same concentration of nanoparticles obtained for suspensions of ciprofloxacin-loaded mucosomes. This procedure was used both for freeze-dried and non-freeze-dried nanoparticles.

Preparation of Ciprofloxacin for the treatment
A stock solution of ciprofloxacin was prepared by dissolving the powder at the final concentration of 4096 µg/mL in DMSO at 96 °C. The stock solution was then diluted to 512 µg/mL in MH, and lower concentrations were obtained through serial dilutions in MH.

Bacterial strains and culture conditions

The bacterial strains used in the study were the Gram-negative *Pseudomonas aeruginosa (P. aeruginosa)* PAO1 and the Gram-positive *Staphylococcus aureus (S. aureus)* ATCC 25,923. Bacteria were respectively inoculated in 10 mL of MH (Catalogue #70192, Merck, DE) and grown overnight at 37 °C, under aerobic conditions, using a shaker incubator (VDRL Stirrer 711/CT, Asal S.r.l., Milan, Italy). Fluorescent *P. aeruginosa* PAO1 and *S. aureus* strains, expressing respectively mCherry and DsRed fluorescent proteins, were also used in the study. The fluorescent strains were grown in MH broth supplemented with antibiotic: carbenicillin (300 µg/mL) (CAS #4800-94-6, Merck, DE) for mCherry-expressing *P. aeruginosa* and chloramphenicol (10 µg/mL) (CAS #56-75-7, Merck, DE) for DsRed-expressing *S. aureus*[10].

The number of bacterial colony-forming units (CFUs/mL) to use in the experiments was determined by comparing the optical density (OD600) of the sample, measured through a UV/VIS spectrophotometer, with a standard curve relating the OD to bacterial CFU/mL[35].

In vitro bacterial planktonic culture assays

According to the European Committee on Antimicrobial Susceptibility Testing (EUCAST) guidelines for the identification of the minimal inhibitory concentration of treatment (MIC), two types of assays were performed in planktonic growth conditions: the agar diffusion test and the dose-dependent effects of mucosomes compared to the free ciprofloxacin.

Agar diffusion test
MH-agar plates were prepared using 90 mm Petri dishes. 5 mL of bacterial suspensions (10^5 CFUs/mL) were plated on MH-agar. After the suspension was completely adsorbed by the agar, a disc of adsorbent paper (5 mm in diameter) was placed in the plate, and 10 µL of treatment (ciprofloxacin-loaded mucosomes or free ciprofloxacin, at 1024, 512, and 256 µg/mL) was pipetted on it. The efficacy of the treatments was evaluated by measuring the radius of the inhibition circle after 24 h at 37 °C[36].

Dose-dependent effects of mucosomes

100 µL of bacteria (10^4 CFUs/mL) were seeded in a 96-well plate. 100 µL of treatment (empty mucosomes, ciprofloxacin-loaded mucosomes, and free ciprofloxacin) in the concentration range 512 –0.5 µg/mL were added to each well, and the plate was incubated for 24 h at 37 °C. Bacteria seeded in tissue culture plate (TCP) wells, without treatment, were considered as positive controls. After incubation, bacterial viability was evaluated through the quantitative 3-[4,5-dimethylthiazol-2-yl]-2,5-diphenyltetrazolium bromide (MTT) assay (Sigma Aldrich, St Louis, MO, USA) as previously described[35]. The colorimetric reaction was analyzed with a CLARIOstar plate reader (BMG Labtech, Ortenberg, Germany) at 570 nm with 630 nm as reference wavelength. A titration curve was used to relate the absorbance to CFUs/mL. The survival rate was calculated by dividing the number of viable bacteria after treatments by the number of viable bacteria in untreated samples (TCP).

Antibacterial efficacy of freeze-dried mucosomes

After their synthesis, ciprofloxacin-loaded mucosomes were freeze-dried and stored at 4 °C for up to 14 days. Before being used, mucosome suspensions were reconstituted to their original volume by resuspending the freeze-dried pellet in PBS. The antibacterial activity of freeze-dried and resuspended mucosomes was evaluated for 3 different ciprofloxacin concentrations (0.03 µg/mL, 4.00 µg/mL, and 64.00 µg/mL for *P. aeruginosa* and 0.03 µg/mL, 0.50 µg/mL, and 64.00 µg/mL for *S. aureus*) using the methods described in Sect. "Dose-dependent effects of mucosomes". Viability was expressed as a percentage of the untreated control, according to Eq. 4.

$$Viability = 100 \times \frac{OD_{570-630}\ (Sample)}{OD_{570-630}\ (Untreated\ control)} \tag{4}$$

In vitro antibiofilm assay

Biofilms treatment

The experiments were performed under two treatment conditions for both bacterial strains: biofilm inhibition and eradication treatments. Overnight cultures of *P. aeruginosa* and *S. aureus* were diluted to 10^7 CFUs/mL in MH containing 1% glucose for *P. aeruginosa* and 0.25% for *S. aureus*[35].

Biofilm inhibition treatments (pre-biofilm condition). Aliquots of 100 µL of the diluted bacterial suspensions were seeded in 96-well culture plates (Euroclone S.p.a, Italy), and incubated for 24 h at 37 °C with 100 µL of treatment (empty mucosomes, ciprofloxacin-loaded mucosomes, and ciprofloxacin) in the concentration range 512 –0.5 µg/mL. Tissue culture plate (TCP) wells used as positive controls and represented by untreated biofilms were included in the experiment.

Bacterial biofilm viability was quantitatively evaluated with the MTT colorimetric assay as previously described (Sect. "Dose-dependent effects of mucosomes"). A titration curve was used to relate the absorbance to CFUs/mL. The surviving fraction was determined by dividing the number of viable bacteria after treatment by the number of viable bacteria in untreated controls (TCP wells).

Biofilm eradication treatments (post-biofilm condition). 200 µL of *P. aeruginosa* and *S. aureus* bacteria, cultured in glucose-supplemented media as aforementioned, were seeded in a 96-well plate for 24 h at 37 °C. At the end of the incubation period, the supernatant containing planktonic cells was carefully removed, and 100 µL of either empty mucosomes, ciprofloxacin-loaded mucosomes, or free ciprofloxacin was added to the previously formed biofilms. After 24 h of incubation, the supernatant was carefully removed, and the biofilms were gently washed with sterile PBS. The formed biofilms were vigorously disrupted, and the bacterial cell viability was quantitatively measured through the MTT assay as previously reported. A titration curve was used to relate the absorbance to CFUs/mL. The surviving fraction was determined by dividing the number of viable bacteria after treatment by the number of viable bacteria in untreated controls (TCP wells).

Biofilm biomass quantification (crystal violet assay). Bacterial biofilm formation was evaluated using the Crystal Violet (CV) assay, following a previously established protocol[37]. Briefly, biofilms were gently washed twice with sterile PBS 1X to remove non-adherent planktonic bacteria. The remaining biofilms were fixed with 96% ethanol for 10 min and then stained with 0.1% crystal violet for 15 min. After multiple washing steps, the wells were let dry. To quantify biofilm formation, the bound dye was solubilized using 10% glacial acetic acid, and absorbance was measured at 590 nm using CLARIOstar (BMG Labtech, Ortenberg, Germany). Results are shown in the Supporting Information expressed as absorbance values for both bacterial strains tested.

Confocal laser scanning microscopy (CLSM) imaging

To perform CLSM measures, 200 µL of both bacterial strains were seeded on sterile glass coverslips placed inside 48-well plates and incubated for 24 h at 37 °C. Biofilms were treated with the biofilm inhibitory concentration (BIC)[38,39]. After the incubation, the supernatants were removed, and the biofilms were carefully washed with sterile PBS. The viability of the bacterial cells in treated biofilms was monitored using the LIVE/DEAD® BacLight bacterial viability kit as described previously[40]. This kit uses SYTO9 fluorescent nucleic acid to stain viable cells (in green) and propidium iodide to stain dead cells (in red). In addition, the produced biofilm matrix was stained in blue with the fluorescent tracer molecule EbbaBiolight 480 (Ebba480, Ebba Biotech, Stockholm, Sweden), diluted 1:1000 in the overnight cultures. Finally, stained bacteria were analyzed with a Leica CLSM (model TCS SP8 DLS; Leica, Wetzlar, Germany) with a 63X oil immersion objective. The excitation and emission wavelengths used for monitoring SYTO9 were 488 and 525 nm, respectively. Propidium iodide was excited at 520 nm, and its emission was monitored at 620 nm. For EbbaBiolight 480, excitation and emission wavelengths were 420 nm and 480 nm, respectively. The orthogonal projections and 3D reconstructions were acquired on 5 ($n = 5$) regions of interest. Scale bars were generated using the LAS X software. The fluorescence intensity of the red, green, and blue channels of the 5 acquired images was evaluated using FIJI software as previously described[41,42].

Scanning electron microscopy (SEM) imaging
After the incubation time, the planktonic bacteria were removed and the biofilms were washed carefully with PBS 1X, fixed with 2.5% (v/v) glutaraldehyde (Sigma-Aldrich, St. Louis, SM, United States), and treated as previously described[40]. SEM images were acquired on 5 ($n=5$) regions of interest, using a Zeiss EVO-MA10 scanning electron microscope (Carl Zeiss, Oberkochen, Germany), 20 kV acceleration voltage, were acquired at 6k× and 15k× magnifications, with scale bars of 2 µm and 1 µm, respectively.

Treatment efficacy through a mucus-mimicking interface

A previously established model mimicking the composition and viscoelastic properties of human pathologic pulmonary mucus was used to assess treatment effectiveness[12]. Transwell® plates were prepared as described in Sect. "Permeability assessment through a mucus-like membrane". 600 µL of bacteria (10^4 CFUs/mL) were inoculated in the donor well of a 24-well plate. The gel-loaded insert was then added, and 200 µL of treatment (ciprofloxacin-loaded mucosomes or free ciprofloxacin) (500 µM) were loaded in the insert (donor compartment). The system was then incubated at 37 °C for 24 h before measuring the viability with the MTT assay as described in Sect. "Antibacterial efficacy of freeze-dried mucosomes". Viability was expressed as a percentage of the untreated control, according to Eq. 4.

Hemolytic activity

Agar blood test. Bacteria (10^4 CFUs/mL) were inoculated on agar blood plate kindly provided by Roberta Migliavacca (Department of Clinical Surgical, Diagnostic and Pediatric Sciences, University of Pavia, Italy) to evaluate the hemolysis. Mucosomes (empty and ciprofloxacin-loaded) were inoculated as well to determine the hemolytic activity. After inoculation of *P. aeruginosa* and *S. aureus* bacteria and mucosomes on different agar blood plates, they were incubated overnight at 37 °C[43]. Results are shown in the Supporting Information.

Hemolysis assay. Human blood obtained from healthy donors was provided by Fondazione IRCCS Policlinico San Matteo, Pavia (Italy), and isolated according to the Italian national policies (see Sect. Ethics). The experiment was performed as described previously[44]. In brief, blood obtained from two donors was centrifuged at 1700x *g* for 5 min. The pellet was washed three times with PBS 1x. After the last wash, the erythrocytes were resuspended 1:100 in PBS to obtain a solution of 1%. In a 96-well plate, 100 µL of the solution was dispensed and incubated with 100 µL of different concentrations [512 –0.25 µg/mL] of mucosomes (empty and drug-loaded). PBS was used as the negative control, and 10% Triton X-100 was used as a positive control of hemolysis. The plates were incubated for 1 h at 37 °C. After the incubation time, plates were centrifuged at 1700x *g* for 5 min, and the supernatant was transferred into a clean 96-well plate, and the absorbance was read at 405 nm through a CLARIOstar reader. The experiment was performed in triplicate. Results are shown in the Supporting Information.

Phagocytic assay of mucosome-treated bacterial biofilms

To assess the effect of mucosome treatments combined with phagocytosis on the disruption and survival of bacterial specimens, biofilms were subjected to the different mucosomes treatments, followed by incubation with human blood[45]. Human blood obtained from healthy donors was provided by Fondazione IRCCS Policlinico San Matteo, Pavia (Italy), and isolated according to the Italian national policies (see Sect. Ethics).

To perform the experiments, *P. aeruginosa* and *S. aureus* strains were seeded for 24 h at 37 °C in post-biofilm conditions as previously described. After the removal of supernatant, biofilms were treated with 200 µL of fresh blood obtained from six healthy donors. BIC concentrations (*P. aeruginosa* 64 µg/mL and *S. aureus* 32 µg/mL)[38,39] were used: 50 µL of ciprofloxacin, ciprofloxacin-loaded mucosomes, and empty mucosomes suspensions were immediately added to each well. Plates were incubated at 37 °C with gentle shaking, and after 3 h, serial dilutions were plated on MH-agar plates to determine the number of surviving CFUs. Control wells consisted of untreated biofilms (without blood), supplemented with 250 µL of PBS. Additional PBS control wells, consisting of biofilms incubated with the different mucosomes treatments, have been introduced. Results were represented as survival rate versus control, represented by the untreated biofilms in PBS.

Mucosomes-bacteria interactions in a 3D model of mucosal infection

CF-Mu^{3}Gel (Bac^{3}Gel Lda., PT) was used to establish 3D models of *P. aeruginosa* or *S. aureus* pulmonary infection[10]. CF-Mu^{3}Gel relies on a hydrogel produced starting from a blend of sodium alginate and porcine gastric mucin type III. Mucin is first dissolved in Müller-Hinton at a concentration equal to 25 mg/mL. Sodium alginate is then dissolved in the mucin solution at a final concentration equal to 5% (w/v). The crosslinking is later induced by diffusing calcium ions for 24 h from a 0.16% (w/v) solution of calcium gluconate (Sigma-Aldrich, DE) through a 0.4 µm polyester membrane (WHA70604704, Sigma-Aldrich, DE). This process allows the production of hydrogels with CF-mucus-like viscoelastic properties, which are characterized by an O_2 gradient that mimics the one measured for CF mucus. The procedure to produce CF-Mu^{3}Gel is protected by an Italian patent (IT102018000020242A). The substrates were inoculated with 100 µL of bacterial suspension at a concentration of 10^4 cells/mL and incubated at 37 °C. After 24 h, the supernatant was removed, and 100 µL of treatment (ciprofloxacin-loaded mucosomes or free ciprofloxacin) in the concentration range [512 – 0.5] µg/mL were added, then the system was incubated at 37 °C. After 24 h, the supernatant was removed, the hydrogels were dissolved using a specific formulation supplied by Bac^{3}Gel Lda., and viability analyses were performed with the MTT assay as previously described.

A similar set-up was exploited to study the interactions between bacteria and mucosomes. To this end, the CF-Mu^{3}Gel substrates were inoculated with 100 µL of fluorescent bacterial suspension at a concentration of 10^4 cells/mL and incubated at 37 °C. After 24 h, the supernatant was removed, and 100 µL of FITC-loaded mucosomes were added at a concentration of nanoparticles corresponding to the one at which the MIC was previously identified, and the system was incubated at 37 °C. After 24 h, the supernatant was removed, the gels

were retrieved from the plate, washed with isotonic NaCl solution, and observed with a confocal-laser-scanning-microscope (SP8, Leica, DE), with a 40× oil-immersion objective (Leica, DE). Fluorescence observations were performed using peak excitation and emission wavelengths of mCherry, DsRed, and FITC.

Statistical analysis

All the experiments were performed in triplicate on at least 2 independent batches. The statistical analysis and the representation of plots were performed using GraphPad Prism 9 (GraphPad Inc., San Diego, CA, United States). For the statistical analyses, the Student t-test or the Mann-Whitney test was employed for pairwise comparison, depending on whether the data were distributed normally or not. One-way ANOVA with Bonferroni correction was used for grouped analyses. Significance is represented in the plots depending on the *p*-value (ns: $p > 0.05$; *: $p < 0.05$; **: $p < 0.01$; ***: $p < 0.001$; ****: $p < 0.0001$).

Results

Mucosomes enable the controlled release of Ciprofloxacin

The employed one-pot synthesis led to the production of ciprofloxacin-loaded mucosomes. TEM images revealed that the produced nanoparticles have quasi-spherical morphology, with a diameter ranging between 104 and 145 nm (Fig. 1a). Quantification of ciprofloxacin in the supernatants showed an entrapment efficiency equal to 56 ± 5% (Supplementary Fig. 1). The release of the active principle from mucosomes was characterized by a logarithmic trend, reaching a plateau after ∼ 20 h. Approximately 75% of the original amount of active principle was released at this time point (Fig. 1b). Finally, by loading ciprofloxacin into mucosomes, it was possible to significantly increase the sedimentation time of the suspension, leading to negligible sedimentation after 3 h (Fig. 1c).

Physico-chemical characterization of mucosomes

The characterization of mucosomes in water dispersion (10 mM NaCl) was performed using Asymmetric Flow Field-Flow Fractionation (AF4) coupled with a set of in-line and at-line detectors, including static light scattering (SLS), dynamic light scattering (DLS), and nanoparticle tracking analysis (NTA) (Table 1, Supplementary Fig. 2). The presence of ciprofloxacin had a very small effect on mucosome size and virtually none on their morphology: we recorded a minor shrinkage in the radius of gyration (90 ± 6 nm vs. 115 ± 5 nm; $\overline{(R\_(g, w))}$ via in-line SLS) and in the hydrodynamic radius (95 ± 3 nm vs.130 ± 15 nm; $\overline{(R\_(h, w))}$ via in-line DLS. 85 ± 1 nm vs. 95 ± 2 nm; $\overline{(R\_(h, n))}$ via batch NTA), but the shape factor ($\overline{(R\_(g, w))}/\overline{(R\_(h, w))}$) was indistinguishable for the two formulations. These consistent values across techniques confirm the dimensional robustness of the system. Of note, batch NTA suggests the loading procedure to produce mucosomes at a lower concentration (4.3 ± 0.06 vs. $2.9 \pm 0.3 \times 10^{10}$ particles/mL); this may be primarily due to filtration, and in any case did not significantly affect size distribution/morphology (Figure SI 2).

Mucosomes preserve the antimicrobial activity of Ciprofloxacin and enhance its activity against planktonic cultures of *S. aureus*

Agar diffusion tests revealed a dose-dependent trend of the inhibition radius dimension for both *P. aeruginosa* (Fig. 2a) and *S. aureus* (Fig. 2b). At the tested concentrations, no statistically significant differences were recorded when treating *P. aeruginosa* and *S. aureus* with either ciprofloxacin-loaded mucosomes or free ciprofloxacin (Fig. 2a and b). A further detail on the inhibition radius is provided in Supplementary Fig. 3. By testing the dose-dependent effect of empty mucosomes, it was possible to observe that the nanoparticles expressed an intrinsic ability to limit bacterial growth. For *P. aeruginosa* (Fig. 2c), a significant decrease in viability compared to the untreated control was found starting from a treatment concentration equal to 64 μg/mL. For *S. aureus* (Fig. 2d), a similar effect was observed starting from a treatment concentration equal to 1 μg/mL. The results from a comprehensive dose-dependency experiment (Supplementary Fig. 4) allowed to identify the MIC of each treatment for both *P. aeruginosa* (0.25 μg/mL for ciprofloxacin-loaded mucosomes and free ciprofloxacin) and *S. aureus* (0.25 μg/mL for ciprofloxacin-loaded mucosomes and 0.50 μg/mL for free ciprofloxacin). In these experiments, when ciprofloxacin-loaded mucosomes were used to treat planktonic cultures, no significant differences in terms of efficacy were observed against *P. aeruginosa*, both at the MIC (Fig. 2e) and at the maximum employed concentration (Fig. 2f). Conversely, *S. aureus* displayed a higher susceptibility to ciprofloxacin when it was administered through mucosomes. A significantly stronger activity ($p < 0.01$) was recorded at the MIC (Fig. 2g), as well as at the maximum employed concentration (Fig. 2h).

Freeze-drying and resuspension of ciprofloxacin-loaded mucosomes do not alter their activity

Freeze-drying the ciprofloxacin-loaded mucosomes and storing them at 4 °C for up to 2 weeks before resuspension and usage did not affect their antimicrobial activity. Indeed, no significant differences were reported between the survival rates of *P. aeruginosa* (Fig. 3a) and *S. aureus* (Fig. 3b) depending on the treatment type. The overall comparison with the treatments employed in this work is reported in Supplementary Fig. 4.

Mucosomes can prevent *P. aeruginosa* and *S. aureus* biofilm formation

Experiments performed to evaluate the ability of mucosomes (both empty and loaded with ciprofloxacin) to interfere with biofilm formation are shown in Fig. 4. Regarding *P. aeruginosa*, quantitative dose-dependent experiments performed using the MTT assay (Fig. 4a) demonstrate that ciprofloxacin-loaded mucosomes are more effective than free antibiotics against *P. aeruginosa* biofilms compared to the untreated control (set at 100% biofilm viability, represented by the orange line). Biofilm viability was dose-dependently reduced by approximately 2 logs using ciprofloxacin-loaded mucosomes and antibiotic concentrations higher than

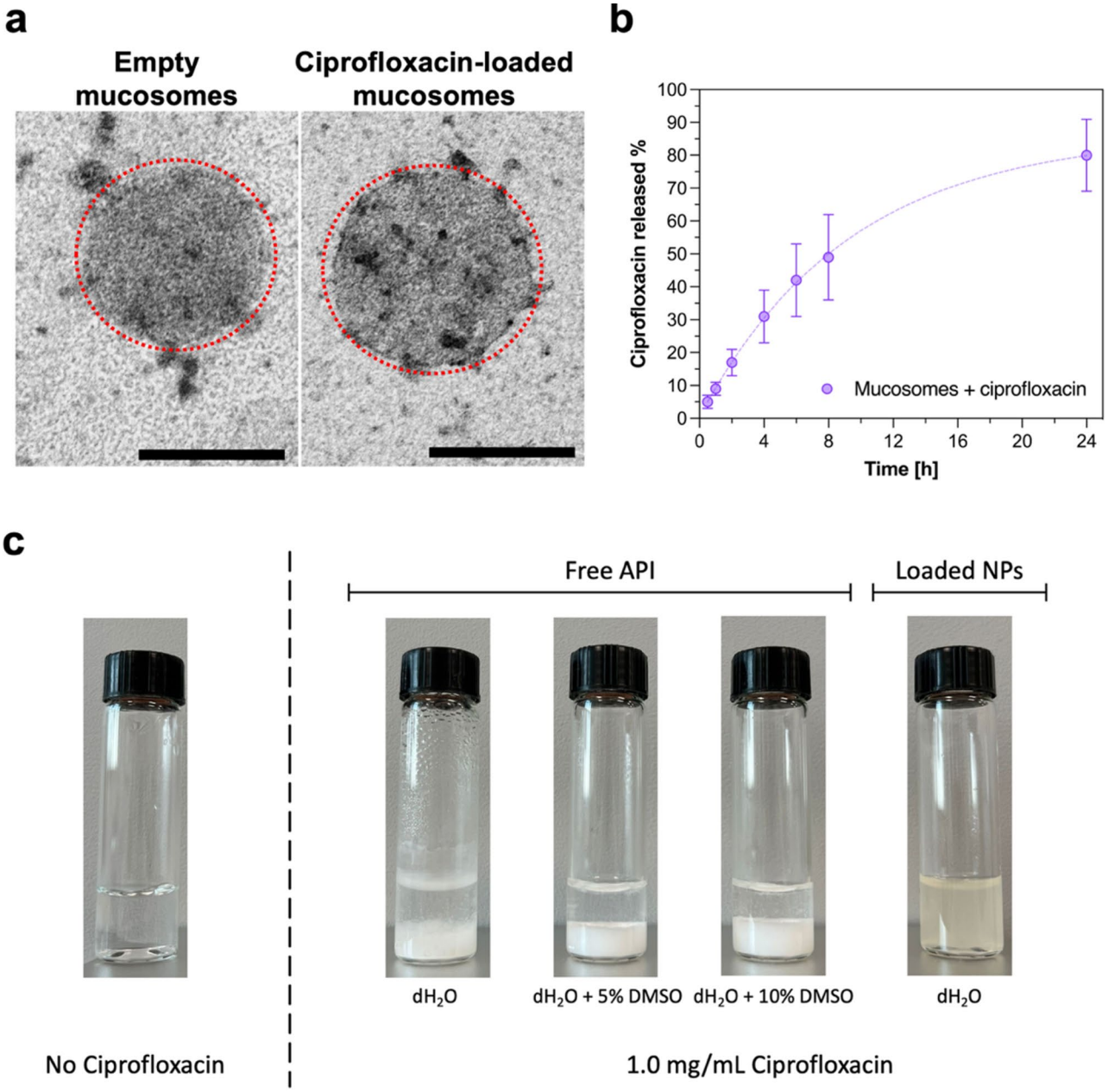

Fig. 1. Characterization of the ciprofloxacin-loaded mucosomes. (**a**) Transmission electron microscopy images representing the size and the morphology of both empty and ciprofloxacin-loaded mucosomes; images acquired at 100 k× magnification (scale bar = 200 nm). The red dashed circumference was added subsequently to better highlight the perimeter of mucosomes. (**b**) Release kinetics of ciprofloxacin from mucosomes into PBS at pH = 7.4. c) Photograph taken 3 h after suspending free ciprofloxacin (1.0 mg/mL) in different solvents (dH_2O with or without 5% or 10% DMSO), showing noticeable Active Pharmaceutical Ingredient sedimentation in the free ciprofloxacin samples, in contrast to the absence of deposition in cipro-loaded NP suspensions.

64 μg/mL, a value considered the minimum required to inhibit *P. aeruginosa* biofilms (BIC). Treatment with antibiotic-loaded mucosomes was consistently more effective than treatment with free ciprofloxacin, reducing bacterial biofilm viability by approximately 1 log at concentrations of ≥ 64 μg/mL (BIC). In contrast, empty mucosomes only reduced biofilm viability by around 0.5 log compared to the untreated control (orange line) at the highest concentration used (512 μg/mL). Qualitative analyses, represented by acquisition of SEM (Fig. 4b) and CLSM (Fig. 4c) images with BIC concentration supported quantitative data. SEM images of *P. aeruginosa* (4b) showed a well-formed biofilm (*control*) and when the mucosomes (empty and drug-loaded) are added in pre-biofilm conditions, they are able to prevent the biofilm formation, as well as free ciprofloxacin. In addition, the morphology of the bacteria in the presence of antibiotics (free or loaded in mucosomes) is altered, suggesting that the antibiotics induce bacterial death. Figure 4c reports CLSM 3D images, demonstrating that empty

	Radius of gyration, $\bar{R}_{g,w}$ (in-line SLS, nm)[a]	Hydrodynamic radius, $\bar{R}_{h,w}$ (in-line DLS, nm)[b]	Shape factor $\bar{R}_{g,w}/\bar{R}_{h,w}$[c]	Hydrodynamic radius, $\bar{R}_{h,n}$ (batch NTA, nm)[d]	Concentration (batch NTA, 10^{10} particles /mL)[e]
Unloaded	115 ± 5	130 ± 15	0.9 ± 0.1	85 ± 1	4.3 ± 0.06
Ciprofloxacin	90 ± 6	95 ± 3	0.9 ± 0.2	95 ± 2	2.9 ± 0.3

Table 1. Physico-chemical characterisation of hydrated loaded and unloaded mucosomes. [a]Weight-average radius of gyration obtained by using SLS and refractive index on-line detectors during AF4 analysis. $n = 3$ measurements of the same sample. [b]Weight-average hydrodynamic radius obtained by using DLS as an on-line detector during AF4 analysis. $n = 3$ measurements of the same sample. [c]Shape factor obtained as the ratio of the values of radius of gyration and hydrodynamic radius see a and b). [d]Number-average hydrodynamic radius obtained by using batch NTA $n = 3$ measurements of the same sample. [e]Number concentration of particles (number of particles per volume unit), $n = 3$ measurements on the same sample.

mucosomes can interfere with biofilm formation, as evidenced by the presence of a dishomogeneous biofilm matrix (cyan) with respect to biofilm control. When the ciprofloxacin-loaded mucosomes are added, they not only prevent the formation of biofilms but also kill bacteria, as observed by bacteria stained in red. In addition, the average of the fluorescence intensity of the biomass (blue channel), determined from 5 CLSM images, was reported in Fig. 4d. The panel showed a significant decrease in fluorescence in the sample with drug-loaded mucosomes.

The effect of mucosomes in preventing the formation of *S. aureus* biofilm is reported in Fig. 4e-h. Figure 4e shows a similar dose-dependent trend for free antibiotic and ciprofloxacin-loaded mucosomes, both reducing biofilm viability of about 0.5 log at 32 μg/mL (*S. aureus* BIC value), compared to the untreated control (set as 100% of biofilm viability - orange line). Moreover, at the highest concentration (512 μg/mL), the ciprofloxacin-loaded mucosomes showed a higher efficacy compared to free antibiotics. Empty mucosomes showed, instead, to slightly reduce *S. aureus* biofilm viability only at the highest concentration. These quantitative results are supported by both SEM (Fig. 4f) and CLSM analyses (Fig. 4g), indicating that the different treatments prevent both *S. aureus* and *P. aeruginosa* from forming biofilm.

From qualitative SEM and CLSM images of both bacterial biofilm controls is possible to notice the disparate thickness of biofilm biomass, which is higher in *S. aureus* than *P. aeruginosa*. These data are coherent with the crystal violet assay, performed to evaluate quantitatively the biomass produced by both bacteria (Supplementary Fig. 5). CLSM orthogonal projections of the bacterial biofilm samples, untreated and treated with antibiotics and mucosomes, are reported in Supplementary Fig. 6.

Furthermore, Table 2 reports the thickness values of both bacterial biofilms, untreated and in the different conditions. These values were determined from CLSM 3D projections (Figs. 4c-g) and, as previously stated, the data on biofilm' controls support those regarding the biomass production determined through crystal violet (Supplementary Fig. 5).

Mucosomes can disrupt *P. aeruginosa* and *S. aureus* established biofilm

The effect of empty and ciprofloxacin-loaded mucosomes to disrupt pre-formed bacterial biofilms was evaluated quantitatively through MTT assay (Fig. 5a-e), and data were supported by SEM and CLSM analyses (Fig. 5b-d; f-h). Quantitative measurements performed on *P. aeruginosa* biofilm (Fig. 5a) revealed that antibiotic-loaded mucosomes, at BIC concentration (64 μg/mL), reduced biofilm viability of approximately 1.5-log, concerning free ciprofloxacin, which showed a reduction of ca. 0.5-log. In addition, they reduced the biofilm viability of almost 2-logs at the highest concentration used (512 μg/mL), in comparison to free antibiotics that showed about a 1-log reduction. Empty mucosomes were shown to slightly disrupt a pre-formed biofilm at 64 μg/mL and with a progressive increase of their anti-biofilm activity at 512 μg/mL (reduction of ca. 0.5-log). Quantitative data were supported by SEM (Fig. 5b) and CLSM (Fig. 5c-d) analyses that showed the disruption of biofilm after the addition of empty mucosomes, and when the antibiotics are free or inside the nanoparticles, it can kill the neighboring bacteria. The antibiofilm activity is higher in ciprofloxacin-loaded mucosomes, as further supported by the analysis of fluorescence intensity of the biofilm matrix-blue channel (Fig. 5d).

The antibiofilm activity of mucosomes against *S. aureus* is reported in Fig. 5e-h. Data shows that ciprofloxacin-loaded mucosomes have a higher effect on biofilm than free drugs (Fig. 5e). The reduction of biofilm viability is of ca. 0.5-log at 32 μg/mL (BIC value), and it increases to ca. > 1-log at the highest concentration tested (512 μg/mL). Empty mucosomes showed a slight reduction only at the highest concentration. SEM images of *S. aureus* biofilm (Fig. 5f) treated with BIC concentration supported the results that all the treatments caused a disintegration of the tightly packed biofilm matrix, formed in the untreated control. Moreover, *S. aureus* morphology was altered when the biofilm was treated with ciprofloxacin-loaded mucosomes. CLSM 3D (Fig. 5g), orthogonal projections (Supplementary Fig. 7), and the quantification of fluorescence intensity (Fig. 5h) are coherent the obtained quantitative data (Fig. 5e).

In addition, from the post-biofilm condition experiments, it was observed that the minimal biofilm eradication concentration (MBEC) for both bacterial biofilms is > 512 μg/mL.

Furthermore, the thickness of both bacterial biofilms after the various treatments was retrieved from CLSM analysis, and the values are shown in Table 3. As reported in the table and supported by the data of biomass formation (Supplementary Fig. 5), Gram-positive untreated biofilm is thicker than Gram-negative's. Moreover, the addition of the various treatments, mainly ciprofloxacin-loaded mucosomes, reduces them by roughly 50%.

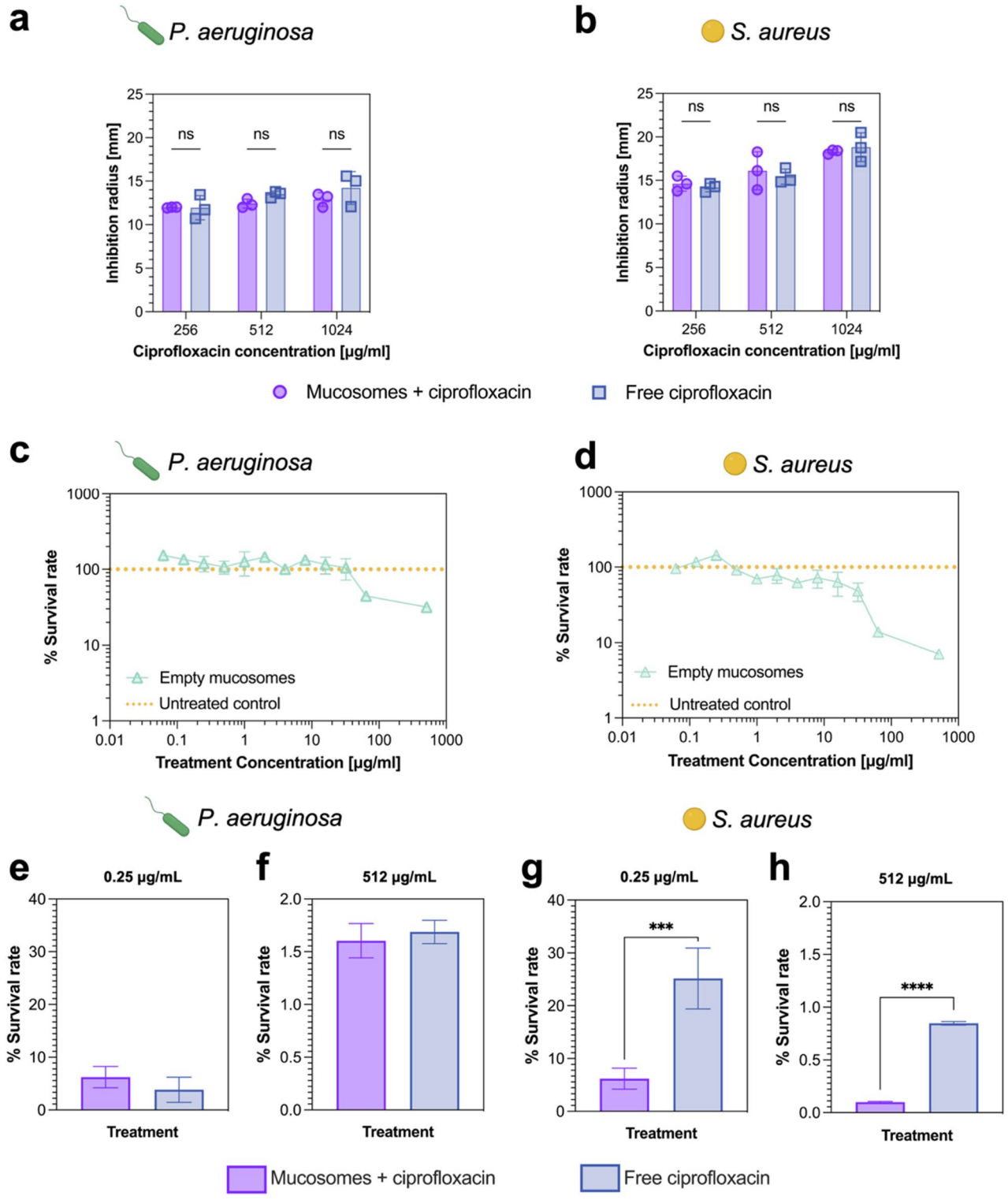

Fig. 2. Efficacy of ciprofloxacin-loaded mucosomes against planktonic cultures of *P. aeruginosa* and *S. aureus*. Results expressed in terms of inhibition radius for the agar diffusion tests performed on (**a**) *P. aeruginosa* and (**b**) *S. aureus*. Empty mucosomes were found effective in limiting the growth of (**c**) *P. aeruginosa* and (**d**) *S. aureus* starting from a treatment concentration of 64 μg/mL and 1.0 μg/mL, respectively (these values indicate the concentration of ciprofloxacin that would be delivered by the employed amount of mucosomes if they were loaded with drug). When *P. aeruginosa* was treated with ciprofloxacin-loaded mucosomes, no significant differences between the efficacy of the mucosomal formulation and the free active principle. (**e**) At a MIC-equivalent concentration (0.25 μg/mL) and (**f**) at higher concentrations (512 μg/mL). Conversely, ciprofloxacin-loaded mucosomes were found to be more effective than free ciprofloxacin against *S. aureus*, both (**g**) at the MIC-equivalent concentrations (0.50 μg/mL), as well as at h) higher concentrations (512 μg/mL).

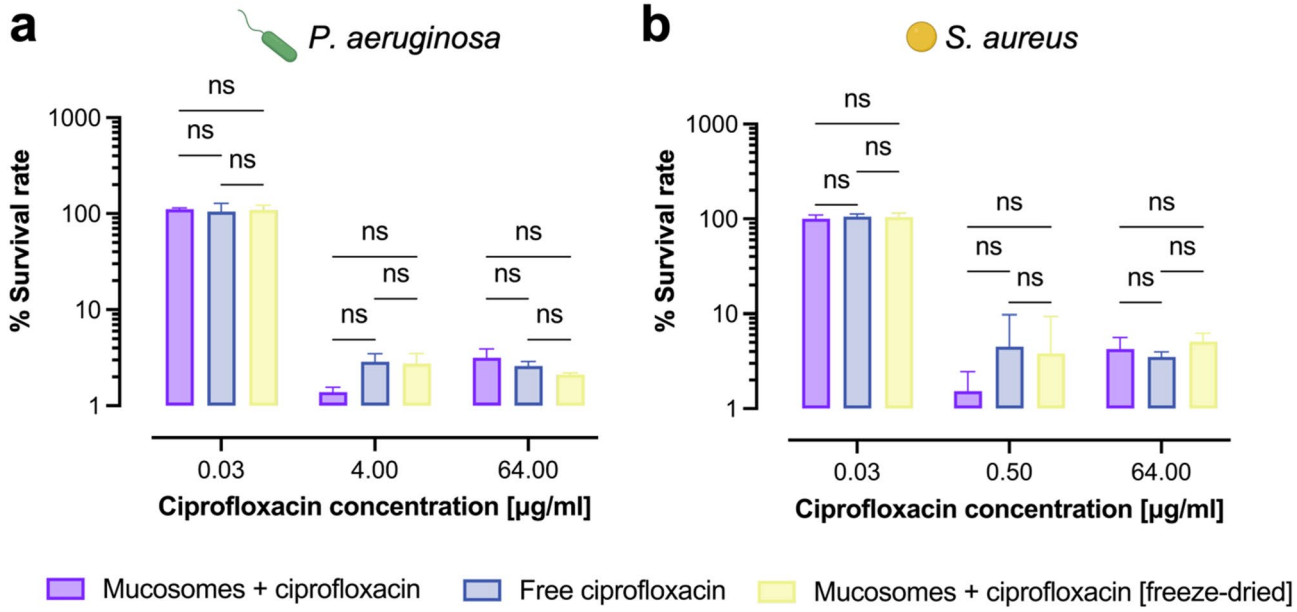

Fig. 3. Ciprofloxacin-loaded mucosomes can be freeze-dried and stored before being used. No differences in terms of antibacterial efficacy were found for (**a**) *P. aeruginosa* and (**b**) *S. aureus*, when comparing the survival rate of the cultures to freeze-dried and rehydrated ciprofloxacin-loaded mucosomes, ciprofloxacin-loaded mucosomes, and free ciprofloxacin. The concentrations of active principle used for this experiment were chosen as the minimum concentration employed in this work, the MIC of ciprofloxacin according to the EUCAST database, and the maximum concentration among those used in this work at which all the treatments showed the same efficacy on both bacterial strains.

Mucosomes improve the antimicrobial efficacy of Ciprofloxacin at mucosal interfaces

The estimation of apparent permeability of mucosomes through a mucus-mimicking hydrogel (Fig. 6a) highlighted the ability of the nanoparticles to enhance the diffusion of ciprofloxacin through a mucus-*like* interface (Fig. 6b). A significant decrease in terms of apparent permeability coefficient (P_{app}) was found when ciprofloxacin was administered through the mucus-mimicking hydrogel, compared to the control. Such a difference was not found when ciprofloxacin-loaded mucosomes were administered. Coherently, the P_{app} of free ciprofloxacin through the gel was found to be significantly smaller than the one estimated for ciprofloxacin-loaded mucosomes. Moreover, when bacteria were grown in the acceptor compartment, results indicated that the survival rates of both *P. aeruginosa* (Fig. 6c) and *S. aureus* (Fig. 6d) to ciprofloxacin-loaded mucosomes were significantly lower than the one measured for free ciprofloxacin (on average 1.7% and 2.4% survival rates were recorded, respectively).

Ciprofloxacin-loaded mucosomes synergize with blood-resident macrophages to eradicate established biofilms of *P. aeruginosa* and *S. aureus*

Before conducting whole blood experiments, a hemolysis assay was performed to evaluate the hemocompatibility of both empty and ciprofloxacin-loaded mucosomes with human red blood cells. No hemolytic activity was observed for these mucin-based nanoparticles, supporting their compatibility with erythrocytes. Data are shown in Supplementary Fig. 8. Based on these results, we devised an additional strategy whereby bacterial biofilms could be dispersed by mucosomes and then subjected to phagocytosis in whole blood.

Biofilms from each strain were exposed to whole blood obtained from six healthy donors and simultaneously treated with free ciprofloxacin, ciprofloxacin-loaded mucosomes, or empty mucosomes. Results from phagocytic assay of mucosomes-treated bacterial biofilms revealed that all treatments were more effective against *P. aeruginosa* (Fig. 7a) and *S. aureus* (Fig. 7b), compared to the untreated control in PBS (CTRL). Both bacterial biofilms treated exclusively with blood exhibited donor-dependent antimicrobial activity, suggesting inter-individual variability as highlighted by lighter red shades in the data visualization relative to the control.

In donors whose blood showed limited antimicrobial activity against *S. aureus* (e.g., donors 5 and 6), the supplementation with empty mucosomes enhanced the eradication of staphylococcal biofilm. Notably, supplementation with ciprofloxacin-loaded mucosomes demonstrated a strong synergistic effect against both pathogens, as indicated by the lightest shades in the color scale. Interestingly, the synergistic effect of drug-loaded mucosomes with blood has been shown to boost the eradication of *P. aeruginosa* biofilms.

Mucosomes target bacterial clusters in a 3D model of pulmonary mucus infection

Three-dimensional cultures of *P. aeruginosa* and *S. aureus*, expressing mCherry and DsRed, respectively, were established within a pathologic in vitro model of pulmonary mucus (CF-Mu^{3}Gel). Cultures were treated with FITC-loaded mucosomes to monitor their spatial distribution within the mucus-mimetic matrix. Both

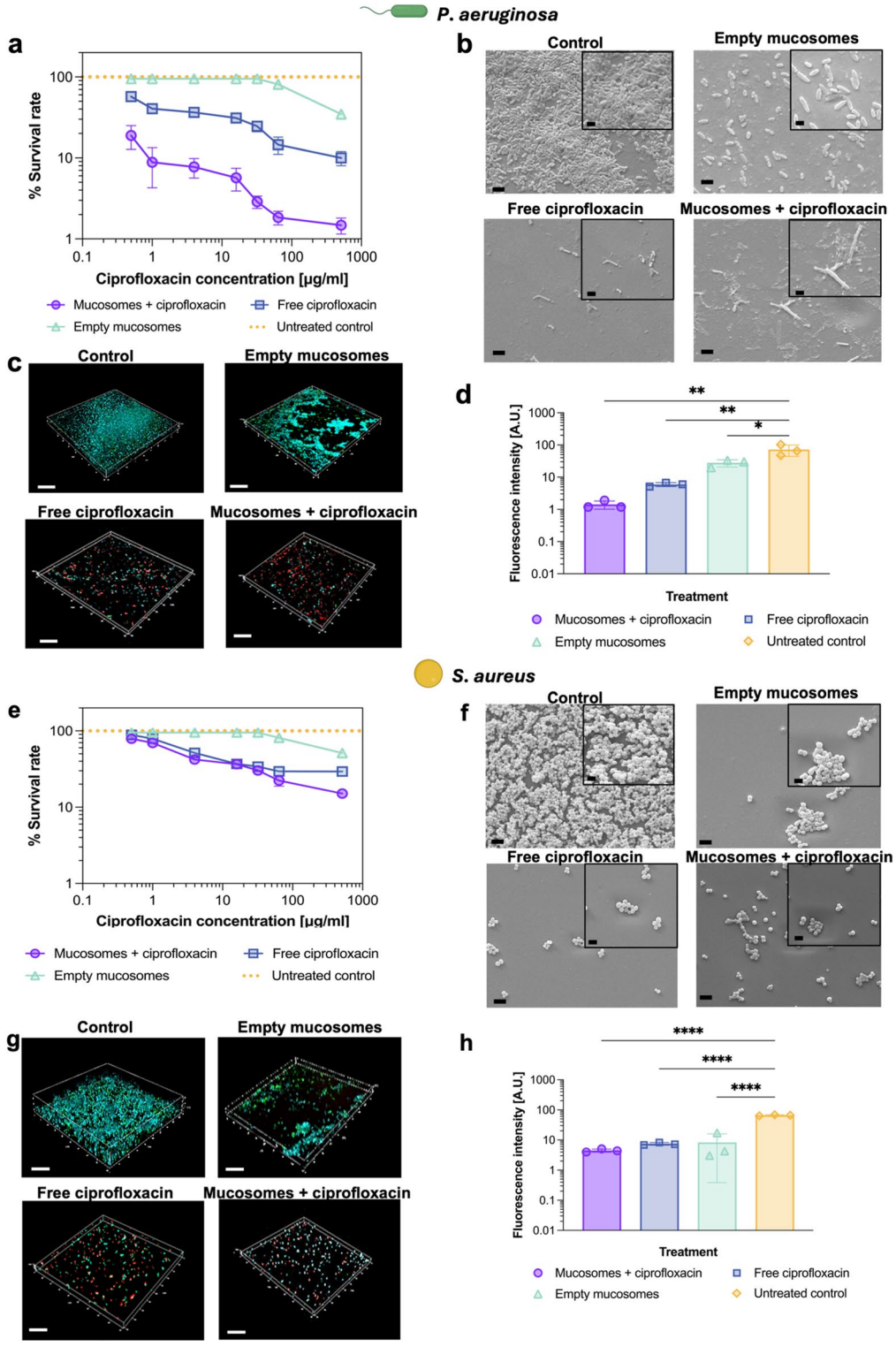

Fig. 4. Evaluation of the ability of mucosomes to prevent biofilm formation. (**a**, **e**) Dose-dependent quantitative effect of each treatment on *P. aeruginosa* (**a**) and *S. aureus* (**e**). (**b**, **f**) SEM on *P. aeruginosa* (**b**) and *S. aureus* (**f**) biofilms. Images acquired at 6k× magnification (scale bars = 2 µm), insets at 15k× (scale bar = 1 µm). (**c**, **g**) CLSM 3D projections of *P. aeruginosa* (**c**) and *S. aureus* (**g**) biofilms. The images acquired at 63× magnification (scale bars = 50 µm) highlight the biofilm matrix (stained in cyan), viable bacteria (stained in green), and dead bacteria (stained in red). (**d**, **h**) Quantification of the blue-channel fluorescence intensity for *P. aeruginosa* (**d**) and *S. aureus* (**h**) biofilms from CLSM acquisitions.

P. aeruginosa				*S. aureus*			
Control	Free ciprofloxacin	Empty mucosomes	Mucosomes + ciprofloxacin	Control	Free ciprofloxacin	Empty mucosomes	Mucosomes + ciprofloxacin
8 µm	4.5 µm	4.5 µm	5 µm	25 µm	12 µm	13 µm	9 µm

Table 2. Thickness of the biofilm layer measured from CLSM acquisition on samples treated in biofilm-forming conditions.

P. aeruginosa (Fig. 8a) and FITC-loaded mucosomes (Fig. 8b) formed heterogeneous clusters with maximum widths of ≈ 27 µm and ≈ 15 µm, respectively, with overlapping signals in several regions (Fig. 8c). Similarly, *S. aureus* cultures formed clusters of a maximum dimension of ≈ 19 µm (Fig. 8d), and multiple aggregates of FITC-loaded mucosomes (Fig. 8e) were observed in overlapping regions (Fig. 8f).

Controls highlighted the colocalization between mucosomes and bacteria, as well as the organization of well-formed clusters of mucosomes in the proximity of bacterial aggregates that were not caused by mucosomes aggregating spontaneously (Supplementary Fig. 9a). Similarly, FITC clusters were not detectable when FITC alone was incubated with *P. aeruginosa* and *S. aureus* (Supplementary Fig. 9b and 9c).

Discussion

The pace at which bacterial infections are outrunning the currently available treatments represents a severe concern to humankind[46]. The development of novel antibiotics is nowadays not an appealing strategy to Pharma companies as the rise of rapid resistance could jeopardize the efforts sustained[4,5,47]. Among the various alternative strategies to fight bacterial infections is the administration of already available antibiotic drugs through tailored nanocarriers[48–50]. This approach aims to increase the efficacy of already-approved medications while exploiting synergistic effects with the carrier. Different options to produce nanocarriers for drug delivery have been proposed recently[51,52]. Among these, glycosylated mucin nanoparticles (mucosomes) represent promising candidates thanks to their unique properties, especially in the context of mucus-related infections[34]. Secreted mucins are the major non-aqueous, bioactive component of human mucus, and their role in representing the first line of defense of the organism has been thoroughly documented[53]. Structurally, mucins are densely glycosylated oligomeric glycoproteins, presenting the characteristic mucin domains where the protein backbone is decorated with *O*-glycans. After secretion, mucins assemble into a tridimensional net that behaves as a barrier against environmental threats through size and chemical filtering. Specifically, mucin glycans can act as decoys for pathogens such as bacteria and viruses that selectively bind the glycans in the initial phase of infection[8,9,54–56]. Previous observations showed how *P. aeruginosa* and *S. aureus* can bind mucin through multiple surface receptors and structures. These include flagella, flagellar cap proteins, and lectins for *P. aeruginosa* and sialoprotein-binding proteins, lectin-*like* proteins, and wall teichoic acids for *S. aureus*[57–62].

Such an elegant defense mechanism inspired the use of mucosomes as an offensive tool to fight bacterial infections[34]. The possibility of loading mucosomes with ciprofloxacin is the first novel aspect described in this paper. Thanks to their unique mucoadhesiveness, we envisioned mucosomes as game-changers for the inhalatory administration of ciprofloxacin. Ciprofloxacin is a broad-spectrum fluoroquinolone antibiotic that is effective against both Gram-negative and Gram-positive bacteria, by interfering with DNA replication[63]. Thanks to its lipophilicity, ciprofloxacin can permeate the lipopolysaccharide barrier of Gram-negative bacteria and finally target DNA gyrase. On the other hand, in Gram-positive bacteria, this antibiotic inhibits topoisomerase IV, which is critical for DNA segregation during cell division[64].

Considering these, ciprofloxacin has the potential to be formulated as an inhalable antibiotic to fight pulmonary infections. In this way, it could directly target the site of infection, thus reducing risks and side effects connected to other administration routes[63,65]. Unfortunately, this application of ciprofloxacin is challenged by its low solubility and permeability (BCS class IV compound)[66,67]. Moreover, without a proper carrier, ciprofloxacin would be rapidly cleared from the pulmonary mucosa, requiring repeated administration on a daily basis that would end up impacting patient compliance[68–70].

Our results indicate that mucosomes are suitable for ciprofloxacin delivery. Mucosomes, whether unloaded or loaded with ciprofloxacin, show very similar physical characteristics. Firstly, in terms of size, they are nanoparticles in the 90–130 nm range (Table 1); secondly, their identical shape factor of 0.9 shows a similar internal structure, more specifically the same mass distribution. Thirdly, this value may lead us to describe these mucosomes as 'soft spheres', but the presence of large-size "tails" in DLS (Supplementary Fig. 2) may lead to overestimate $R_{h,w}$, thus the actual shape factor may actually be > 1, which would signal an anisotropic mass distribution such as that of an elongated structure. Indeed, mucins have been reported to adopt dumbbell-shaped or "pearl necklace" morphologies, which would be compatible with the shape factor values observed here[71,72]. The suitability of mucosomes as drug carriers is further highlighted by the possibility to achieve the controlled release of ciprofloxacin from mucosomes.

This fact, together with the strong reproducibility of dose-dependent trends against planktonic bacteria, indicates that mucosomal formulations of ciprofloxacin are suitable to bypass the solubility-related issue of this molecule. In addition to these benefits, the advantageous effects of using mucosomes to deliver ciprofloxacin were already evident in the simplest infection models (i.e., in agar plates and 2D planktonic cultures). We show how ciprofloxacin-loaded mucosomes preserve ciprofloxacin's activity when incubated with *P. aeruginosa* and *S. aureus* planktonic and biofilm cultures. In our work, we demonstrated that empty mucosomes can interfere with biofilm formation and disaggregate a pre-existing biofilm. Consequently, a collaborative effort involving mucin-based nanoparticles loaded with ciprofloxacin has been shown to enhance antibacterial activity. When

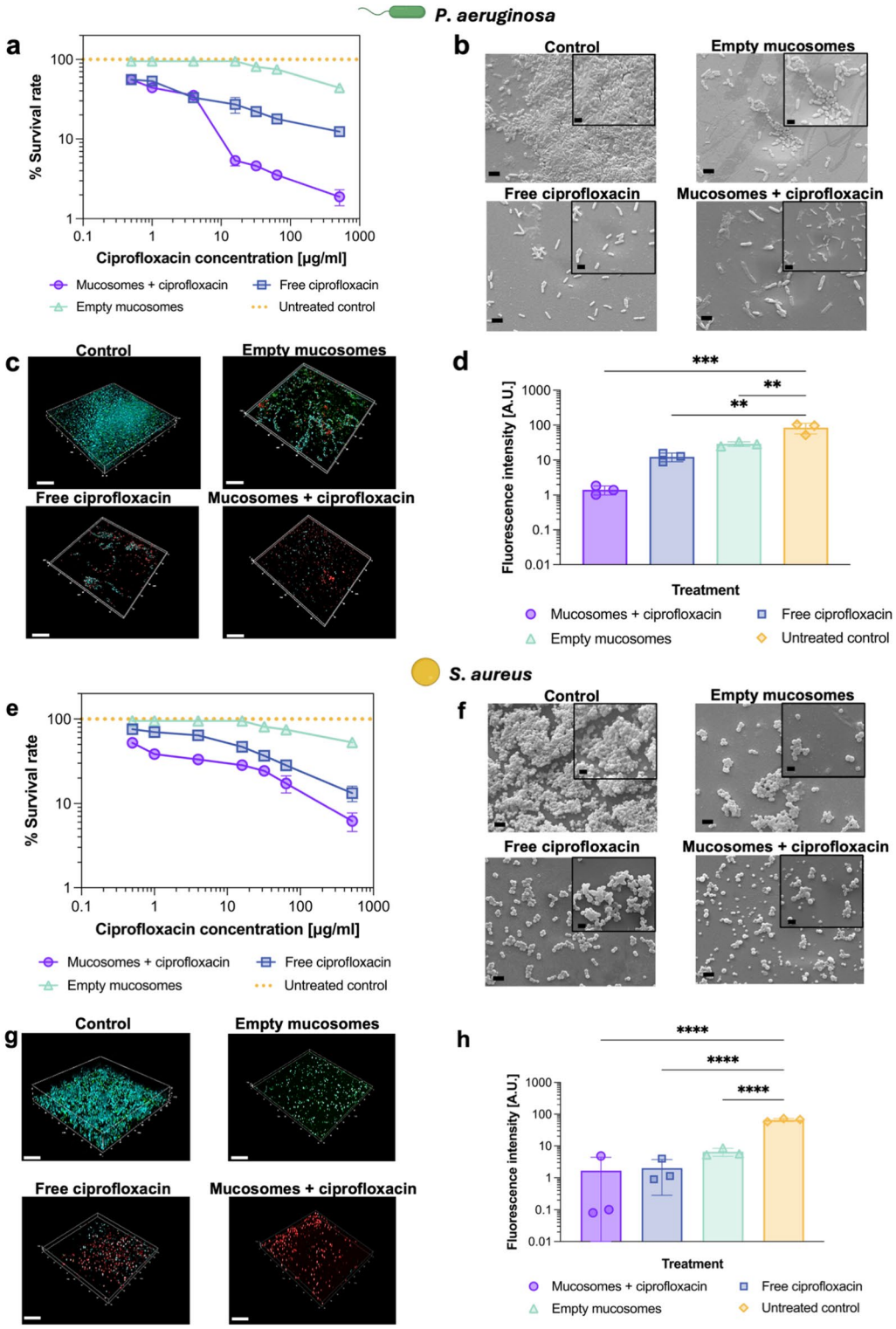

Fig. 5. Evaluation of the ability of mucosomes to disrupt established biofilms. (**a**, **e**) Dose-dependent quantitative effect of each treatment on *P. aeruginosa* (**a**) and *S. aureus* (**e**) biofilms. (**b**, **f**) SEM on *P. aeruginosa* (**b**) and *S. aureus* (**f**) biofilms. Images acquired at 6k× magnification (scale bars = 2 µm), insets at 15k× (scale bar = 1 µm). (**c**, **g**) CLSM 3D projections of *P. aeruginosa* (**c**) and *S. aureus* (**g**) biofilms. The images acquired at 63× magnification (scale bars = 50 µm) highlight the biofilm matrix (stained in blue), viable bacteria (stained in green), and dead bacteria (stained in red). (**d**, **h**) Quantification of the blue-channel fluorescence intensity for *P. aeruginosa* (**d**) and *S. aureus* (**h**) biofilms from CLSM acquisitions.

P. aeruginosa				*S. aureus*			
Control	Free ciprofloxacin	Empty mucosomes	Mucosomes + ciprofloxacin	Control	Free ciprofloxacin	Empty mucosomes	Mucosomes + ciprofloxacin
8 µm	4.5 µm	4.5 µm	4.5 µm	25 µm	16 µm	12 µm	12 µm

Table 3. Thickness of the biofilm layer measured from CLSM acquisitions on samples that were treated after biofilm establishment.

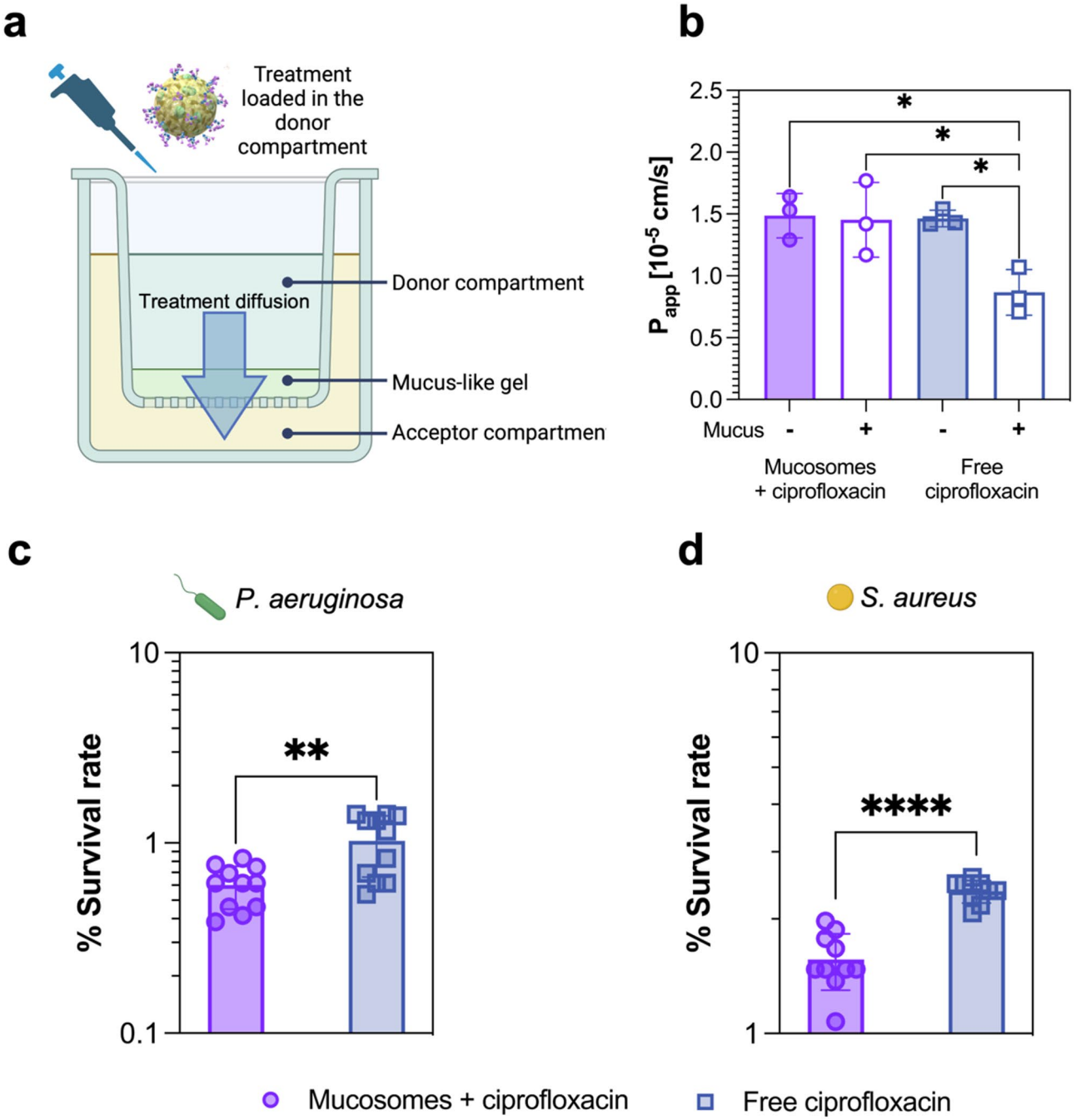

Fig. 6. Mucosomes enhance the delivery of ciprofloxacin through a mucus-like interface. (**a**) Schematization of the experimental set-up. (**b**) When ciprofloxacin was loaded into mucosomes, the presence of a mucus-mimicking interface did not alter its diffusion into the acceptor compartment. The survival rate of (**c**) *P. aeruginosa* and (**d**) *S. aureus* significantly decreases ($p < 0.001$ for *P. aeruginosa* and $p < 0.00001$ for *S. aureus*) when the cultures are treated with ciprofloxacin-loaded mucosomes, compared to free ciprofloxacin.

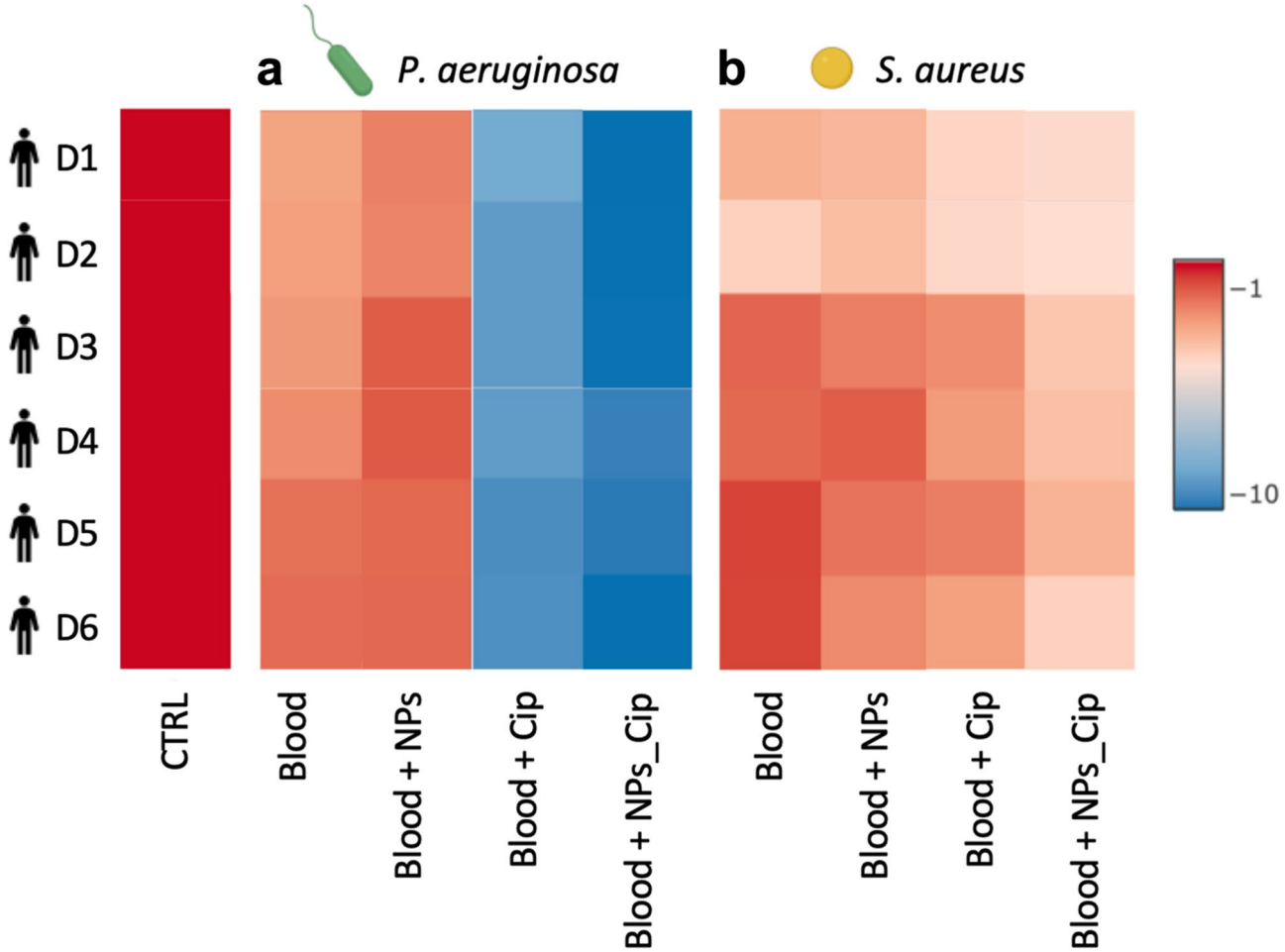

Fig. 7. The synergistic effect between mucosomes and human blood in eradicating *P. aeruginosa* and *S. aureus* biofilms. Heat map illustration of the logarithmic decrease in (**a**) *P. aeruginosa* and (**b**) *S. aureus* viability following treatment with blood samples from six human healthy donors, as well as with blood enriched with empty mucosomes (NPs), free ciprofloxacin (Cip), and ciprofloxacin-loaded mucosomes (NPs_Cip). All data for both bacterial strains were statistically significant vs. CTRL (P value < 0.05).

administered to planktonic cultures of *S. aureus*, ciprofloxacin-loaded mucosomes improved the effectiveness of the free antibiotic, leading to a significant decrease in the observed MIC. The different activity of drug-loaded mucosomes on bacteria can be attributed primarily to the distinctions between Gram-positive and Gram-negative bacteria, and their activation of resistance mechanisms[73]. Differences are predominantly manifested in the cell wall, which is thicker in *S. aureus* (Gram-positive). *P. aeruginosa* exhibits, instead, a thinner cell wall and an external cell membrane. Furthermore, *S. aureus* is a sessile bacterium, while *P. aeruginosa* has flagella that allow the bacterium to move in the medium. The discrepancies in planktonic conditions suggest that the interaction between *S. aureus* and ciprofloxacin-loaded mucosomes is more pronounced in the case of the Gram-positive bacteria compared to Gram-negative bacteria, such as *P. aeruginosa*. This phenomenon can be attributed to the Brownian motion phenomenon, which plays a crucial role in such biological processes by facilitating molecular movement[74]. The synergy between the bactericidal effect of ciprofloxacin and the bacteriostatic properties of mucins likely causes this phenomenon[75]. This explanation is further supported by the dose-dependent trend observed for free mucosomes, which can significantly decrease bacterial proliferation in a 24-hour time course.

Mucins are known for their bioactivity in bacterial cultures[75–79]. Recent discoveries related these mucin functions to its glycosylations[80–82]. Mucin glycans were found to be able to modulate bacterial behavior in multiple ways, including decreasing the proliferative power of bacteria and attenuating the virulence of various bacterial strains[80–82]. The preservation of mucin bioactivity after the glycoproteins are assembled into nanoparticles is a novel aspect that confers mucosomes a competitive edge when using them in treating bacterial infections.

During bacterial infections, the formation of biofilms acts as a significant virulence factor by increasing resistance to antibiotics and evading immune defenses, thereby posing a serious threat to human health. Significant efforts are currently being put into finding efficient strategies to deal with biofilms, as they represent a major threat responsible for more than 80% of refractory nosocomial infections[25,83,84]. Indeed, organization within biofilm communities is one of the main strategies adopted by bacteria to resist conventional antibiotic treatments[85,86]. Hence, an additional aspect underlining the positive impact of delivering antimicrobial drugs

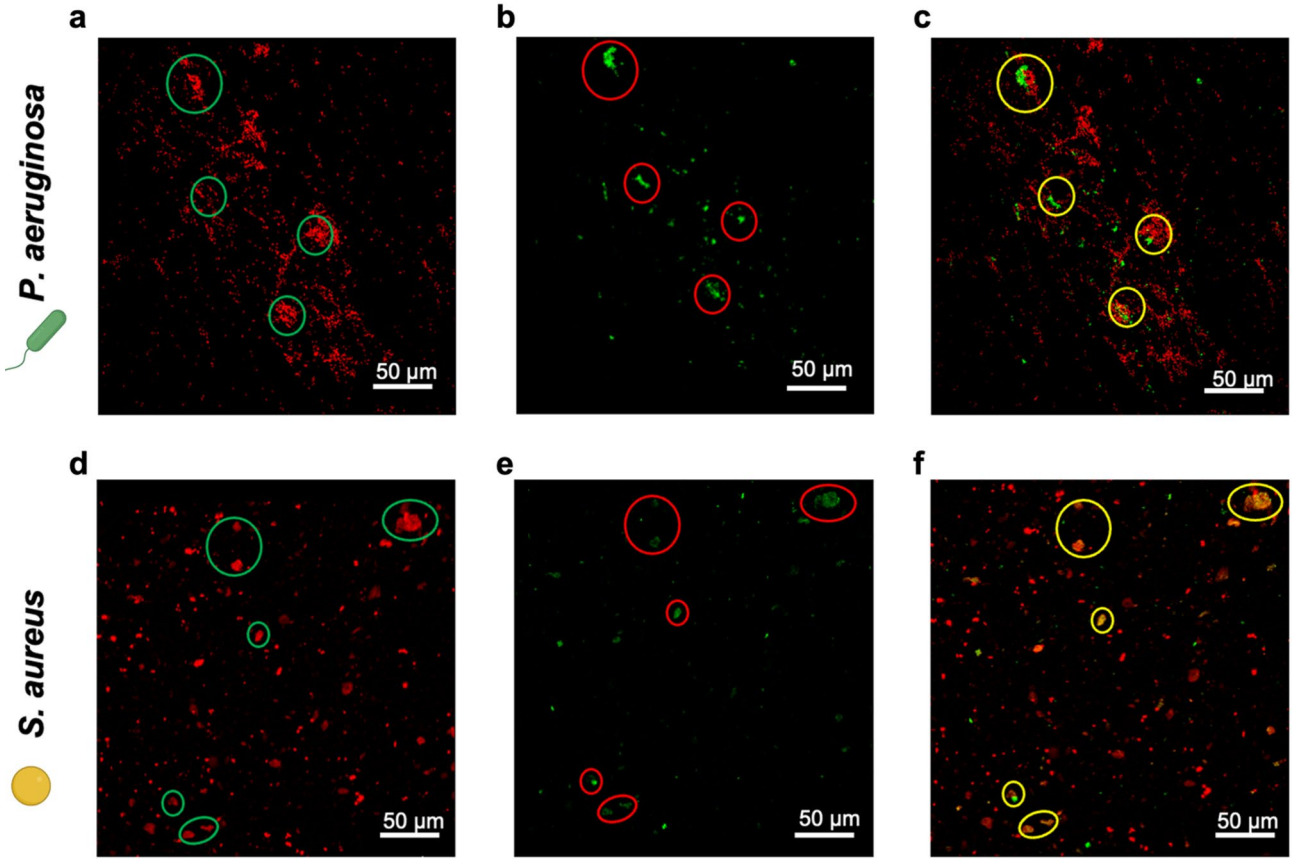

Fig. 8. Mucosomes colocalize with bacteria in a 3D model of pulmonary mucus infection. (**a**) The red channel of the image shows *P. aeruginosa* that was transformed to express red fluorescence (mCherry). From this picture, it is possible to observe the bacterial aggregates (highlighted with green circles) that were formed during the experimental time-course. (**b**) The green channel of the image for *P. aeruginosa* culture shows a non-random distribution of FITC-loaded mucosomes (clusters are highlighted with red circles). (**c**) By merging the red and green channels it is possible to appreciate the co-localization between bacteria clusters and mucosomes (highlighted with green circles). (**d**) Similarly, by looking at the red channel image for *S. aureus* cultures (bacteria were transformed to express DsRed fluorescent protein), it can be noticed that bacteria are organized into multicellular clusters (highlighted with green circles) after 48 h in culture. (**e**) From the green channel image, it is possible to spot different aggregates of mucosomes (highlighted with red circles). (**f**) When merging the 2 channels also for *S. aureus* cultures, mucosomes are preferentially located in the proximity of *S. aureus* clusters. All the scale-bars in this figure are equal to 50 µm.

with mucosomes is represented by their ability of these nanocarriers to actively interact with *P. aeruginosa* and *S. aureus* biofilms. Previous studies reported how mucins can prevent bacterial aggregation into biofilms through a glycan-mediated interaction with bacterial lectins[75,87–89]. Furthermore, exposure to mucin glycans is also known for downregulating the expression of genes related to the production of biofilm[81]. Here, we demonstrate that the antibiofilm properties of mucins are preserved even when mucins are formulated as mucosomes. Mucosomes also improved the efficacy of ciprofloxacin against well-established biofilms of both *P. aeruginosa* and *S. aureus*. Free mucosomes disassembled the biofilm matrix, resulting in an enhanced bactericidal effect of ciprofloxacin. The ability of mucosomes to disperse established biofilm communities was also found crucial to enhance the exposure of bacteria to blood-resident macrophages. This represents an important element when considering the applicability of mucosomes in the clinics[45]. Indeed, the biofilm matrix is not only responsible for shielding the bacteria from administered antibiotics, but it also prevents immune cells from targeting them[90,91].

This biofilm-disassembling behavior was already observed when mucin solutions were administered to in vitro-grown biofilms of both *P. aeruginosa* and *S. aureus* and showed to be caused by the selective binding of mucin glycans to bacteria, which together affected the ability of cells to aggregate and to attach to a surface, favoring the expression of a quasi-planktonic phenotype[75,80,82].

The distinct behavior exhibited by ciprofloxacin-loaded mucosomes on planktonic cultures and biofilms of *P. aeruginosa* is attributable to the motility of bacteria and their interaction with nanoparticles. *P. aeruginosa* is a motile bacterium with flagella that facilitate movement within the medium. Consequently, the hypothesis is that low interactions occur in the planktonic state of bacteria due to Brownian motion[74]. Conversely, when *P. aeruginosa* forms a biofilm, this form is sessile because it is attached to a surface[92]. In such instances, the probability of interaction between biofilms and nanoparticles is high. Furthermore, the thickness of *P. aeruginosa*

biofilms is less substantial than biofilms formed by *S. aureus*. This finding is corroborated by the quantification of biofilm biomass, performed with the Crystal Violet assay (Supplementary Fig. 5), and by biomass dimensional analysis (Tables 2 and 3).

A further characteristic that makes mucosomes optimal for fighting complex bacterial infections is their ability to permeate the mucus layer. Results presented in this work illustrated the ability of mucosomes to permeate different in vitro models of the mucosal interface. This aspect is utterly important, as the efficient transmucosal delivery of antimicrobial drugs might be a game-changer in the treatment of multiple mucus-related disorders[93,94]. In physiological conditions, the clearance mechanism provides a constant turnover of mucus, ensuring the elimination of the entrapped pathogens and air pollutants[95–97]. However, several diseases, including chronic obstructive pulmonary disease, asthma, and cystic fibrosis, are connected to dysfunctions in mucus production or renewal[10,98]. These pathologies are characterized by the alteration of different chemical and physical properties of the mucus that lead to impaired mucociliary clearance, thus causing the unsuccessful expulsion of pathogens that are free to grow in a protected and nutritious environment[10]. In these cases, the mucosal layer stops being the first line of defense of the organism and becomes a safe outpost for the external aggressors that protects them by limiting the diffusion of drugs and by impeding the adequate immune cells activation, thus finally promoting the development of chronic infections[10,99]. Nevertheless, once safely established within the mucus, bacteria might start organizing into biofilm communities, thus further worsening the odds of achieving positive outcomes with traditional pharmacological treatments[53,100].

According to the results presented in this work, mucosomes were not only able to dive through mucus-*like* interfaces to safely deliver their load, but they were also able to selectively target bacteria in a complex environment. This was evident from CLSM images, which highlighted the colocalization between FITC-loaded mucosomes and the major clusters of both *P. aeruginosa* and *S. aureus*. The driver behind this targeting is expected to be the intrinsic glycosylation of mucosomes[34]. Multiple studies described the ability of mucin glycans to selectively link lectins exposed on the external surface of different bacteria[75,87–89,101]. This behavior was not only observed with pathogenic strains but even with probiotic strains like *A. muciniphila* (which populates the gut and takes advantage of mucin glycans as a nourishing source)[102,103]. These known interactions are likely to be the cause of the colocalization observed in the CLSM images.

Freeze-drying has been identified as an effective method to enhance the long-term stability of mucosomes, offering a significant advantage for their clinical application and overcoming the challenges that hinder their potential use in medical therapies. The definition of a strategy to safely store the nanosystem before use was considered a mandatory requirement to ensure its stability and functional integrity prior to application. Indeed, one of the most frequent issues affecting nanosystems for drug delivery is the ability to store them stably, without altering the carrier's properties or the drug's release kinetics[104–107]. In this sense, the results obtained for freeze-dried mucosomes further highlight the translational potential of this nanoparticle.

Finally, to further ensure the hemocompatibility of the developed mucosomes, their hemolytic activity was evaluated. Hemolysis assays are widely used as a preliminary method to evaluate the safety of systemically administered materials, as they reveal a compound's potential to damage red blood cell membranes and trigger the release of intracellular contents. Due to their simplicity, cost-effectiveness, and reproducibility, these assays are considered a standard tool in early cytotoxicity screening[44]. In our study, neither empty nor ciprofloxacin-loaded mucosomes exhibited any detectable hemolytic activity. This confirms their compatibility with erythrocytes and supports their suitability for systemic use in applications involving contact with blood. Building on these findings, we then investigated the synergistic effect of mucosomes on blood phagocytosis against bacterial biofilm. Our results showed the extreme efficacy of the combined action of drug-loaded mucosomes and blood in eradicating the biofilms. Therefore, this nanosystem could represent a novel therapeutic strategy for managing biofilm-associated infections, particularly in cases involving bloodstream infections, endocarditis, or infected medical implants, offering a highly effective, multifaceted approach to target bacterial biofilms and addressing a critical unmet need in modern medicine[108].

Conclusions

In this work, we provided evidence of the suitability of ciprofloxacin-loaded mucosomes to fight *P. aeruginosa* and *S. aureus* using different in vitro models of bacterial infections. Mucosomes were able to preserve the efficacy of the loaded active principle, even after freeze-drying, thus being suitable for long-term storage. The delivery through mucosomes enhanced the efficacy of ciprofloxacin against *S. aureus* by significantly reducing the characteristic minimum inhibitory concentrations of the drug. Mucosomes were able to prevent the formation of *P. aeruginosa* and *S. aureus* biofilms, as well as to disassemble well-established biofilm communities. This behavior synergized with the antimicrobial activity of ciprofloxacin, thus significantly improving the outcomes of the antimicrobial treatment of bacterial biofilms. Mucosomes were also found able to selectively target the studied bacteria when they were grown in a 3D, hydrogel-based model of human mucus, as well as to improve the diffusion of ciprofloxacin through mucus-*like* interfaces.

The efficacy of ciprofloxacin-loaded mucosomes has been further proved to enhance the phagocytic activity of blood against bacterial pre-formed biofilms. In conclusion, mucosomes employment can increase the likelihood of favorable outcomes in the treatment of mucus-resident and blood-stream infections, making this nanosystem an ideal candidate for clinical application.

Data availability

Data are available from the corresponding authors upon reasonable request.

Received: 17 April 2025; Accepted: 3 July 2025

Published online: 25 July 2025

References

1. de Kraker, M. E. A., Stewardson, A. J. & Harbarth, S. Will 10 million people die a year due to antimicrobial resistance by 2050? *PLoS Med.* **13**, e1002184 (2016).
2. Iskandar, K. et al. Antibiotic Discovery and Resistance: The Chase and the Race. *Antibiotics* 11, (2022).
3. Darby, E. M. et al. Molecular mechanisms of antibiotic resistance revisited. *Nature Reviews Microbiology 2022 21:5* 21, 280–295 (2022).
4. MacNair, C. R., Rutherford, S. T. & Tan, M. W. Alternative therapeutic strategies to treat antibiotic-resistant pathogens. *Nature Reviews Microbiology 2023 22:5* 22, 262–275 (2023).
5. Brown, D. Antibiotic resistance breakers: can repurposed drugs fill the antibiotic discovery void? *Nature Reviews Drug Discovery 2015 14:12* 14, 821–832 (2015).
6. Linden, S. K., Sutton, P., Karlsson, N. G., Korolik, V. & McGuckin, M. A. Mucins in the mucosal barrier to infection. *Mucosal Immunol.* **1**, 183–197 (2008).
7. Liu, C. et al. Meta-analysis of mucosal microbiota reveals universal microbial signatures and dysbiosis in gastric carcinogenesis. *Oncogene* **41**, 3599–3610 (2022).
8. Jiang, K. et al. Modulating the bioactivity of mucin hydrogels with crosslinking architecture. *Adv Funct. Mater* **31**, 2008428 (2021).
9. Yan, H. et al. Immune-Informed mucin hydrogels evade fibrotic foreign body response in vivo. *Adv Funct. Mater* **29**, 1902581 (2019).
10. Peneda Pacheco, D. et al. Heterogeneity governs 3D-Cultures of clinically relevant microbial communities. *Adv. Funct. Mater.* **33**, 2306116 (2023).
11. Sardelli, L. et al. Engineering biological gradients: (2019). https://doi.org/10.1177/2280800019829023 17.
12. Pacheco, D. P. et al. Disassembling the complexity of mucus barriers to develop a fast screening tool for early drug discovery. *J. Mater. Chem. B.* **7**, 4940–4952 (2019).
13. Kretschmer, M. et al. Synthetic mucin gels with Self-Healing properties augment lubricity and inhibit HIV-1 and HSV-2 transmission. *Advanced Science* **9**, 2203898 (2022).
14. Stoopler, E. T. & Sollecito, T. P. Oral mucosal diseases. *Med. Clin. North Am.* **98**, 1323–1352 (2014).
15. Shah, B. K., Singh, B., Wang, Y., Xie, S. & Wang, C. Mucus hypersecretion in chronic obstructive pulmonary disease and its treatment. *Mediators Inflamm.* **2023**, 1–15 (2023).
16. The Lancet Respiratory Medicine. New developments in bronchiectasis. *Lancet Respir Med.* **11**, 755 (2023).
17. Yang, R., Wu, X., Gounni, A. S. & Xie, J. Mucus hypersecretion in chronic obstructive pulmonary disease: from molecular mechanisms to treatment. *J. Transl Int. Med.* **11**, 312–315 (2023).
18. Pedersoli, L. et al. Engineered modular microphysiological models of the human airway clearance phenomena. *Biotechnol. Bioeng.* **118**, 3898–3913 (2021).
19. Lyczak, J. B., Cannon, C. L. & Pier, G. B. Lung infections associated with cystic fibrosis. *Clin. Microbiol. Rev.* **15**, 194–222 (2002).
20. Short, B. et al. Informed development of a multi-species biofilm in chronic obstructive pulmonary disease. *APMIS* **132**, 336–347 (2024).
21. Jennings, L. K. et al. Pseudomonas aeruginosa aggregates in cystic fibrosis sputum produce exopolysaccharides that likely impede current therapies. *Cell. Rep.* **34**, 108782 (2021).
22. Karygianni, L., Ren, Z., Koo, H. & Thurnheer, T. Biofilm matrixome: extracellular components in structured microbial communities. *Trends Microbiol.* **28**, 668–681 (2020).
23. Uribe-Querol, E. & Rosales, C. Control of phagocytosis by microbial pathogens. *Front Immunol* **8**, 1368 (2017).
24. Burmølle, M. et al. Enhanced biofilm formation and increased resistance to antimicrobial agents and bacterial invasion are caused by synergistic interactions in multispecies biofilms. *Appl. Environ. Microbiol.* **72**, 3916–3923 (2006).
25. Zhao, A., Sun, J. & Liu, Y. Understanding bacterial biofilms: from definition to treatment strategies. *Front Cell. Infect. Microbiol* **13**, 1137947 (2023).
26. Costerton, J. W., Stewart, P. S. & Greenberg, E. P. Bacterial biofilms: A common cause of persistent infections. *Science* vol. 284 1318–1322 Preprint at (1999). https://doi.org/10.1126/science.284.5418.1318
27. Wu, M., Yang, X., Tian, J., Fan, H. & Zhang, Y. Antibiotic treatment of pulmonary infections: an umbrella review and evidence map. *Front Pharmacol* **12**, 680178 (2021).
28. Hurley, M. N., Prayle, A. P. & Flume, P. Intravenous antibiotics for pulmonary exacerbations in people with cystic fibrosis. *Cochrane Database of Systematic Reviews* (2015). (2017).
29. Miravitlles, M. & Anzueto, A. Chronic respiratory infection in patients with chronic obstructive pulmonary disease: what is the role of antibiotics?? *Int. J. Mol. Sci.* **18**, 1344 (2017).
30. Bandi, S. P., Bhatnagar, S. & Venuganti, V. V. K. Advanced materials for drug delivery across mucosal barriers. *Acta Biomater.* **119**, 13–29 (2021).
31. Sato, H., Yamada, K., Miyake, M. & Onoue, S. Recent advancements in the development of nanocarriers for mucosal drug delivery systems to control oral absorption. *Pharmaceutics* **15**, 2708 (2023).
32. Stie, M. B. et al. A head-to-head comparison of polymer interaction with mucin from Porcine stomach and bovine submaxillary glands. *Sci. Rep.* **14**, 21350 (2024).
33. Arenhoevel, J. et al. Thiolated polyglycerol sulfate as potential mucolytic for muco-obstructive lung diseases. *Biomater. Sci.* **12**, 4376–4385 (2024).
34. Butnarasu, C. et al. Mucosomes: intrinsically mucoadhesive glycosylated mucin nanoparticles as Multi-Drug delivery platform. *Adv. Healthc. Mater.* **11**, 2200340 (2022).
35. Restivo, E. et al. Surface properties of a biocompatible thermoplastic polyurethane and its Anti-Adhesive effect against E. coli and S. aureus. *J. Funct. Biomater.* **15**, 24 (2024).
36. Bonev, B., Hooper, J. & Parisot, J. Principles of assessing bacterial susceptibility to antibiotics using the agar diffusion method. *J. Antimicrob. Chemother.* **61**, 1295–1301 (2008).
37. Christensen, G. D. et al. Adherence of coagulase-negative Staphylococci to plastic tissue culture plates: a quantitative model for the adherence of Staphylococci to medical devices. *J. Clin. Microbiol.* **22**, 996–1006 (1985).
38. Lutz, L., Pereira, D. C., Paiva, R. M., Zavascki, A. P. & Barth, A. L. Macrolides decrease the minimal inhibitory concentration of anti-pseudomonal agents against Pseudomonas aeruginosa from cystic fibrosis patients in biofilm. *BMC Microbiol.* **12**, 196 (2012).
39. Kashef, M. T., Saleh, N. M., Assar, N. H. & Ramadan, M. A. The antimicrobial activity of Ciprofloxacin-Loaded niosomes against Ciprofloxacin-Resistant and Biofilm-Forming Staphylococcus aureus. *Infect. Drug Resist.* **13**, 1619–1629 (2020).
40. Sprio, S. et al. Enhancement of the biological and mechanical performances of sintered hydroxyapatite by multiple ions doping. *Front Mater* **7**, 224 (2020).
41. Schindelin, J. et al. Fiji: an open-source platform for biological-image analysis. *Nature Methods 2012 9:7* 9, 676–682 (2012).
42. Guagliano, G. et al. Bioinspired Bioinks for the fabrication of chemomechanically relevant standalone disease models of hepatic steatosis. *Adv Healthc. Mater* **13**, 2303349 (2024).

43. Latorre-Fernández, J. et al. Evaluation of the double-zone hemolysis (DZH) test for the detection of livestock-associated methicillin-resistant *Staphylococcus aureus*. *Microbiol Spectr* **13**, e0110224 (2025).
44. Sæbø, I., Bjørås, M., Franzyk, H., Helgesen, E. & Booth, J. Optimization of the hemolysis assay for the assessment of cytotoxicity. *Int. J. Mol. Sci.* **24**, 2914 (2023).
45. Di Poto, A., Sbarra, M. S., Provenza, G., Visai, L. & Speziale, P. The effect of photodynamic treatment combined with antibiotic action or host defence mechanisms on Staphylococcus aureus biofilms. *Biomaterials* **30**, 3158–3166 (2009).
46. Kariuki, S. Global burden of antimicrobial resistance and forecasts to 2050. *Lancet* **404**, 1172–1173 (2024).
47. Salmond, G. P. & Welch, M. Antibiotic resistance: adaptive evolution. *Lancet* **372**, S97–S103 (2008).
48. Thamilselvan, G. et al. Polymer based dual drug delivery system for targeted treatment of fluoroquinolone resistant Staphylococcus aureus mediated infections. *Sci. Rep.* **13**, 11373 (2023).
49. Ghosh, R. & De, M. Liposome-Based antibacterial delivery: an emergent approach to combat bacterial infections. *ACS Omega*. **8**, 35442–35451 (2023).
50. Nazli, A. et al. Strategies and progresses for enhancing targeted antibiotic delivery. *Adv. Drug Deliv Rev.* **189**, 114502 (2022).
51. Yeh, Y. C., Huang, T. H., Yang, S. C., Chen, C. C. & Fang, J. Y. Nano-Based drug delivery or targeting to eradicate Bacteria for infection mitigation: A review of recent advances. *Front Chem* **8**, 286 (2020).
52. Wang, C. et al. Nanocarriers for the delivery of antibiotics into cells against intracellular bacterial infection. *Biomater. Sci.* **11**, 432–444 (2023).
53. Olsen, I. Mucus is more than just a physical barrier for trapping oral microorganisms. *J. Oral Microbiol.* **12**, 1788352 (2020).
54. Park, S., Chin-Hun Kuo, J., Reesink, H. L. & Paszek, M. J. Recombinant mucin biotechnology and engineering. *Adv. Drug Deliv Rev.* **193**, 114618 (2023).
55. Yan, H. et al. Immune-Modulating mucin hydrogel microdroplets for the encapsulation of cell and microtissue. *Adv Funct. Mater* **31**, 2105967 (2021).
56. Chen, S. et al. Early osteoimmunomodulation by mucin hydrogels augments the healing and revascularization of rat critical-size calvarial bone defects. *Bioact Mater.* **25**, 176–188 (2023).
57. Arora, S. K., Ritchings, B. W., Almira, E. C., Lory, S. & Ramphal, R. The *Pseudomonas aeruginosa* flagellar cap protein, flid, is responsible for mucin adhesion. *Infect. Immun.* **66**, 1000–1007 (1998).
58. Mistretta, N. et al. Glycosylation of Staphylococcus aureus cell wall teichoic acid is influenced by environmental conditions. *Sci. Rep.* **9**, 3212 (2019).
59. Passos da et al. The Pseudomonas aeruginosa lectin LecB binds to the exopolysaccharide Psl and stabilizes the biofilm matrix. *Nat. Commun.* **10**, 2183 (2019).
60. Wen, Q., Gu, F., Sui, Z., Su, Z. & Yu, T. The process of osteoblastic infection by *Staphylococcus Aureus*. *Int. J. Med. Sci.* **17**, 1327–1332 (2020).
61. Miwa, H. E., Gerken, T. A., Jamison, O. & Tabak, L. A. Isoform-specific O-Glycosylation of osteopontin and bone sialoprotein by polypeptide N-Acetylgalactosaminyltransferase-1. *J. Biol. Chem.* **285**, 1208–1219 (2010).
62. Lakhtin, M. et al. Probiotic Lactobacillus and bifidobacterial lectins against Candida albicans and Staphylococcus aureus clinical strains: new class of the pathogen biofilm destructors. *Probiotics Antimicrob. Proteins*. **2**, 186–196 (2010).
63. Zhang, Y. et al. Microfluidics assembly of inhalable liposomal Ciprofloxacin characterised by an innovative in vitro pulmonary model. *Int. J. Pharm.* **635**, 122667 (2023).
64. Shariati, A. et al. The resistance mechanisms of bacteria against Ciprofloxacin and new approaches for enhancing the efficacy of this antibiotic. *Front Public. Health* **10**, 1025633 (2022).
65. Cipolla, D., Blanchard, J. & Gonda, I. Development of liposomal Ciprofloxacin to treat lung infections. *Pharmaceutics* **8**, 6 (2016).
66. Caço, A. I. et al. Solubility of antibiotics in different solvents. Part II. Non-Hydrochloride forms of Tetracycline and Ciprofloxacin. *Ind. Eng. Chem. Res.* **47**, 8083–8089 (2008).
67. Sharma, P. C., Jain, A., Jain, S., Pahwa, R. & Yar, M. S. Ciprofloxacin: review on developments in synthetic, analytical, and medicinal aspects. *J. Enzyme Inhib. Med. Chem.* **25**, 577–589 (2010).
68. Wong, J. P. et al. Liposome delivery of Ciprofloxacin against intracellular Francisella tularensis infection. *J. Controlled Release*. **92**, 265–273 (2003).
69. Shek, P. N. *Liposomes in Biomedical Applications*vol. 6 (CRC, 1995).
70. Hamblin, K. A., Wong, J. P., Blanchard, J. D. & Atkins, H. S. The potential of liposome-encapsulated Ciprofloxacin as a tularemia therapy. *Front Cell. Infect. Microbiol* **4**, 79 (2014).
71. Almutairi, F. M. et al. Application of recent advances in hydrodynamic methods for characterising mucins in solution. *Eur. Biophys. J.* **45**, 45–54 (2016).
72. Yakubov, G. E., Papagiannopoulos, A., Rat, E., Easton, R. L. & Waigh, T. A. Molecular structure and rheological properties of Short-Side-Chain heavily glycosylated Porcine stomach mucin. *Biomacromolecules* **8**, 3467–3477 (2007).
73. Wang, L., Hu, C. & Shao, L. The antimicrobial activity of nanoparticles: present situation and prospects for the future. *Int. J. Nanomed.* **12**, 1227–1249 (2017).
74. Li, G., Tam, L. K. & X. Tang, J. Amplified effect of brownian motion in bacterial near-surface swimming. *Proc. Natl. Acad. Sci.* **105**, 18355–18359 (2008).
75. Feng, X., Zhang, J., Rodríguez-Serrano, A. F., Huang, J. & Hsing, I. M. Antibiofilm and pH-responsive properties of nature-derived mucin biomaterials and their potentials for chronic wound care. *Matter* https://doi.org/10.1016/j.matt.2024.09.002 (2024).
76. Smith, T. J. et al. A mucin-regulated adhesin determines the Spatial organization and inflammatory character of a bacterial symbiont in the vertebrate gut. *Cell. Host Microbe*. **31**, 1371–1385e6 (2023).
77. Petrou, G. & Crouzier, T. Mucins as multifunctional Building blocks of biomaterials. *Biomater. Sci.* **6**, 2282–2297 (2018).
78. Winkeljann, B. et al. Covalent mucin coatings form stable Anti-Biofouling layers on a broad range of medical polymer materials. *Adv Mater. Interfaces* **7**, 1902069 (2020).
79. Mays, Z. J. S., Chappell, T. C. & Nair, N. U. Quantifying and engineering mucus adhesion of probiotics. *ACS Synth. Biol.* **9**, 356–367 (2020).
80. Jacob, K. M., Hernández-Villamizar, S., Hammer, N. D. & Reguera, G. Mucin-induced surface dispersal of Staphylococcus aureus and Staphylococcus epidermidis via quorum-sensing dependent and independent mechanisms. *mBio* 15, (2024).
81. Wheeler, K. M. et al. Mucin glycans attenuate the virulence of Pseudomonas aeruginosa in infection. *Nat. Microbiol.* **4**, 2146–2154 (2019).
82. Wang, B. X. et al. Mucin glycans signal through the sensor kinase RetS to inhibit Virulence-Associated traits in Pseudomonas aeruginosa. *Curr. Biol.* **31**, 90–102e7 (2021).
83. Choi, V., Rohn, J. L., Stoodley, P., Carugo, D. & Stride, E. Drug delivery strategies for antibiofilm therapy. *Nat. Rev. Microbiol.* **21**, 555–572 (2023).
84. Jamal, M. et al. Bacterial biofilm and associated infections. *J. Chin. Med. Association*. **81**, 7–11 (2018).
85. Grooters, K. E. et al. Strategies for combating antibiotic resistance in bacterial biofilms. *Front Cell. Infect. Microbiol* **14**, 1352273 (2024).
86. Davies, D. Understanding biofilm resistance to antibacterial agents. *Nat. Rev. Drug Discov.* **2**, 114–122 (2003).
87. Han, G. & Vaishnava, S. Mucin-binding adhesins: A key to unlocking the door of mutualism. *Cell. Host Microbe*. **31**, 1254–1256 (2023).

88. Dam, T. K., Edwards, J. L., Kadav, P. D. & Brewer, C. F. Mechanism of mucin recognition by lectins: A thermodynamic study. in 169–185 (2022). https://doi.org/10.1007/978-1-0716-2055-7_10
89. Behren, S. et al. Fucose binding motifs on mucin core glycopeptides impact bacterial lectin Recognition**. *Angewandte Chemie Int. Edition* **62**, e202302437 (2023).
90. Sharma, D., Misba, L. & Khan, A. U. Antibiotics versus biofilm: an emerging battleground in microbial communities. *Antimicrob. Resist. Infect. Control.* **8**, 76 (2019).
91. Shree, P., Singh, C. K., Sodhi, K. K., Surya, J. N. & Singh, D. K. Biofilms: Understanding the structure and contribution towards bacterial resistance in antibiotics. *Med. Microecology*. **16**, 100084 (2023).
92. Giaouris, E., Simões, M. & Dubois-Brissonnet, F. The role of biofilms in the development and dissemination of microbial resistance within the food industry. *Foods* **9**, 816 (2020).
93. Lam, J. K. W. et al. Transmucosal drug administration as an alternative route in palliative and end-of-life care during the COVID-19 pandemic. *Adv. Drug Deliv Rev.* **160**, 234–243 (2020).
94. Butnarasu, C., Garbero, O. V., Petrini, P., Visai, L. & Visentin, S. Permeability assessment of a High-Throughput mucosal platform. *Pharmaceutics* **15**, 380 (2023).
95. King, M. Physiology of mucus clearance. *Paediatr. Respir Rev.* **7**, S212–S214 (2006).
96. Sardelli, L. et al. Towards bioinspired *in vitro* models of intestinal mucus. *RSC Adv.* **9**, 15887–15899 (2019).
97. Gustafsson, J. K. & Johansson, M. E. V. The role of goblet cells and mucus in intestinal homeostasis. *Nat. Rev. Gastroenterol. Hepatol.* **19**, 785–803 (2022).
98. Munkholm, M. & Mortensen, J. Mucociliary clearance: pathophysiological aspects. *Clin. Physiol. Funct. Imaging*. **34**, 171–177 (2014).
99. Oriano, M. et al. The open challenge of in vitro modeling complex and Multi-Microbial communities in Three-Dimensional niches. *Front. Bioeng. Biotechnol.* **8**, 1–17 (2020).
100. Domingue, J. C., Drewes, J. L., Merlo, C. A., Housseau, F. & Sears, C. L. Host responses to mucosal biofilms in the lung and gut. *Mucosal Immunol.* **13**, 413–422 (2020).
101. Elzinga, J. et al. Binding of Akkermansia muciniphila to mucin is O-glycan specific. *Nat. Commun.* **15**, 4582 (2024).
102. Bakshani, C. R. et al. Carbohydrate-active enzymes from Akkermansia muciniphila break down mucin O-glycans to completion. *Nat. Microbiol.* **10**, 585–598 (2025).
103. Derrien, M., Vaughan, E. E., Plugge, C. M. & de Vos, W. M. Akkermansia muciniphila gen. Nov., sp. Nov., a human intestinal mucin-degrading bacterium. *Int. J. Syst. Evol. Microbiol.* **54**, 1469–1476 (2004).
104. Gatto, M. S. & Najahi-Missaoui, W. Lyophilization of nanoparticles, does it really work?? Overview of the current status and challenges. *Int. J. Mol. Sci.* **24**, 14041 (2023).
105. Mitchell, M. J. et al. Engineering precision nanoparticles for drug delivery. *Nat. Rev. Drug Discov.* **20**, 101–124 (2021).
106. Sultana, S. et al. Stability issues and approaches to stabilised nanoparticles based drug delivery system. *J. Drug Target.* **28**, 468–486 (2020).
107. Muthu, M. S. & Feng, S. S. Pharmaceutical stability aspects of nanomedicines. *Nanomedicine* **4**, 857–860 (2009).
108. Jesaitis, A. J. et al. Compromised host defense on *Pseudomonas aeruginosa* biofilms: characterization of neutrophil and biofilm interactions. *J. Immunol.* **171**, 4329–4339 (2003).

Acknowledgements

The authors thank the following members of University of Pavia: Amanda Oldani and Patrizia Vaghi from Centro Grandi Strumenti (https://cgs.unipv.it/eng/) for CLSM analyses and Giovanna Bruni (Department of Chemistry) for SEM analyses. E.R. and L.V. acknowledge Alexander Horswill (Department of Immunology & Microbiology University of Colorado Anschutz School of Medicine) for providing DsRed plasmid. The authors thank Paola Bergamaschi from Centro Lavorazione e Validazione, Servizio di Immunoematologia e Medicina Trasfusionale, Fondazione IRCCS Policlinico San Matteo, Pavia for blood samples.

Author contributions

G.G.: methodology, formal analysis, data curation, investigation, visualization, writing – original draft, writing – review and editing E.P.: investigation, methodology, formal analysis, writing - review and editing. C.S.B.: Investigation, visualization, formal analysis, writing – review and editing. E.R.: investigation, methodology, formal analysis, writing – review, and editing. L.S.: formal analysis, visualization, writing – review and editing. E.F.: formal analysis, writing – review and editing. P.P.: conceptualization, supervision, project administration. N.T. and S.S.: Investigation, methodology, formal analysis. L.V.: conceptualization, supervision, funding acquisition, project administration. S.V.: conceptualization, supervision, funding acquisition, project administration.

Funding

L.V., E.R. and E.P. acknowledge the support from the Italian Ministry of University and Research (MUR) and the University of Pavia through the program "Dipartimenti di Eccellenza 2023–2027". The project has been funded by a PRIN (Progetti di Ricerca di Interesse Nazionale) grant, reference code 20227YWZSZ, awarded in 2022 by L.V. and S.V. and supported by Fondazione Compagnia di San Paolo under the Call "Progetto Trapezio".

Declarations

Competing interests

P.P., L.V., and S.V. are co-founders and Scientific advisors of Bac3Gel lda., Portugal, and are co-inventors of the patent IT102018000020242A "Three-dimensional substrate for microbial cultures". P.P., L.V., and S.V. are co-inventors of the patent IT102020000014908A "Covalently cross-linked glycosylated mucin nanoparticles as systems for the delivery and release of active ingredients and biomolecules". The authors declare no other competing interests.

Ethics

The experiments described in Sect. "Hemolytic activity" and "Phagocytic assay of mucosome-treated bacterial biofilms" included the use of biological materials from human healthy donors. Human blood obtained from healthy donors was provided by Fondazione IRCCS Policlinico San Matteo, Pavia (Italy), and isolated

according to Italian national policies, including "Decreto Ministero della Salute 2 November 2015 n.69" and "Accordo Stato-Regioni n.225/CSR 13 December 2018". The study and all experimental protocols were approved by the Ethics Committee of Fondazione IRCCS Policlinico San Matteo, Pavia (approval number not applicable). All methods were performed in accordance with the relevant guidelines and regulations. Per the Declaration of Helsinki, informed consent was obtained from all donors prior to sample collection.

Additional information

Supplementary Information The online version contains supplementary material available at https://doi.org/10.1038/s41598-025-10496-y.

Correspondence and requests for materials should be addressed to L.V. or S.V.

Reprints and permissions information is available at www.nature.com/reprints.

Publisher's note Springer Nature remains neutral with regard to jurisdictional claims in published maps and institutional affiliations.